

In this competing renewal grant application entitled "Human MRI to 9.4T and Beyond", the emphasis is on "Beyond". The current grant now concluding supported the development of whole body imaging at 7T, and human head imaging to 9.4T. While refinements continue, the aims of demonstrating feasibility of human MRI at these highest field strengths were achieved. The development and advancement of parallel transmit, parallel transmitters, multi-channel transmission line arrays and B1 shimming were key technologies and methodologies to make these feats possible. Now, with the development of two new whole body MR systems, one at 10.5T for the University of Minnesota, and the other at 11.7T for CEA Neurospin in Saclay, France, a pair of new highest field MR systems are scheduled for delivery. As was the case with 7T and 9.4T, and for 3T and 4T before, magnet technology has often preceded radiofrequency technology in the evolution of MRI. Field strength has stepped ahead of our ability to use it, again. The purpose of this proposal is therefore to solve this problem for the world's most powerful magnets. Innovative new radiofrequency technology, coils, method and techniques are proposed for achieving the first head and body images from these unprecedented new fields. This effort is aimed at not only developing advanced technology and techniques required to safely harness the world's most powerful whole body MR magnets for science, but will safely achieve the highest field, highest signal, highest speed images yet.

This application seeks renewal of the grant: "Human MRI to 9.4T and "Beyond." With Human MRI to 9.4T achieved, the effort of this proposal is directed to "Beyond". A renewed grant will develop the radiofrequency technology and knowhow required to acquire the first, whole-body images at 10.5T and 11.7T.

RESEARCH PLAN

A. SPECIFIC AIMS

The objective of this proposal is to advance whole body MRI from 7T and 9.4T to 10.5T and 11.7T. The goal therefore will be to achieve the first whole body human images at these two successive field strengths, safely and successfully. By so doing, the trail will be blazed for the next step in high field NMR facilitated biomedical research. To accomplish this objective, new paradigm shifting technologies and methodologies, some only recently invented, must be developed, implemented and applied. Many new discoveries, inventions, and innovations are undoubtedly ahead as well. New RF technology and protocols will be developed to take advantage of five degrees of freedom in signal excitation and detection at the NMR transduction (RF coil-tissue) interface. Time, space, frequency, phase angle, and magnitude will be modulated to optimize desired signal criteria over targeted regions of interest. These new approaches, facilitated by dramatically shortened Larmor wavelengths and unprecedented signal levels, will validate 10.5T and 11.7T systems for human MRI and may compel advancement to higher fields still. Specifically, these approaches will be developed and applied to the human head and trunk at the highest field strengths currently available for human imaging. To assure not only successful, but safe human application of new methods and technology at magnetic field strengths above the FDA "non-significant risk" status, "safety" is also listed as an Aim of primary importance.

Aim 1. Head Imaging Coil , 10.5T to 11.7T.

- 1.1 Specification and Design for RF coil systems at 450-500MHz
- 1.2 Construction
 - 1.2.1 RF coil systems construction, bench testing
 - 1.2.2 Auto-tuning system construction for driving multi-channel coils at 450-500MHz
 - 1.2.3 Integrated coil amplifiers
- 1.3 Head MRI Testing and Evaluation, 10.5T to 11.7T

Aim 2. Body Imaging Coils, 10.5T to 11.7T.

- 2.1 Specification and Design for RF coil systems at 450-500MHz
- 2.2 Construction
 - 2.2.1 RF coil systems construction, bench testing
 - 2.2.2 Auto-tuning system
 - 2.2.3 Integrated coil amplifiers
- 2.3 Body MRI Testing and Evaluation, 10.5T-11.7T

Aim 3. RF Safety, 10.5T to 11.7T.

- 3.1 Modeling and Design
 - 3.1.1 SAR and temperature modeling in digital porcine models at 450-500 MHz.
 - 3.1.2 SAR and temperature modeling in digital human models at 450-500 MHz.
- 3.2 Testing and Evaluation
 - 3.2.1 Measurement of RF power input vs. temperature in porcine models by fluoroptic thermometry
 - 3.2.2 Determine RF heating data for a priori use in experiment planning.
- 3.3 Safety Assurance Implementation
 - 3.3.1 Build and implement multi-channel MR power monitor
 - 3.3.2 Monitor SAR on all channels, forward and reverse, for multi-channel coils

B. RESEARCH STRATEGY

B.1 Significance

In recognition of the significant role that ultra-high field magnetic resonance (MR) has played and will continue to play in basic biomedical research, the NIH NCRR recently awarded a High End Instrumentation grant to the University of Minnesota, Center for Magnetic Resonance Research (CMRR). The grant (S10RR029672-01) was for the purchase of a custom console (Siemens) and a shielded room to complement a 10.5 Tesla (T), 88cm bore magnet purchased by the University of Minnesota. An October 2011 delivery is scheduled for this console and magnet; the 650 ton shielded room is already being installed. Unavailable commercially however are the radiofrequency coils and related RF front-end technology required to complete this system. Similarly unavailable is the support needed to bring this system to safe and successful operation. Our Neurospin collaborators from the grant now proposed for renewal are in a similar spot with similar needs. They anticipate their 11.7T, 90 cm bore magnet to be reach field in October 2013.

This grant is critical for meeting immediate, specific needs, as well as for a broader need for the advancement of the field. One immediate need is to supply fully integrated and operational RF coil systems for head and body imaging at 450 and 500 MHz (Aims 1 and 2). Aim 3 is to obtain data required for safe operation of these systems for the required FDA Investigational Device Exemption, and for the University of Minnesota's IRB approval which must precede human experiments. Neurospin will require the same data for meeting their safety and regulatory criteria for human studies at 11.7T. More broadly, this investigation develops the means to explore the feasibility for the first whole body imaging at the highest field strengths yet.

In the last two decades numerous magnetic resonance techniques, such as functional magnetic resonance imaging (fMRI) (1-13), perfusion imaging (14-18), MR spectroscopy (19-27), etc. have come to play an indispensable role in biomedical research, as well as in clinical practice. In our laboratory, the Center for Magnetic Resonance Research (CMRR) at the University of Minnesota, the evolution of such methods has been intricately tied with the development of high field MR, starting with one of the original three 4T magnets in 1990. This was followed by the installation of a 7 tesla whole body system in 1999 (the first such system), ultimately leading to the rapidly growing interest in 7 T both in the research community and the manufacturers of clinical MR platforms. Based on the dramatic improvements that can be realized at the ultrahigh fields due to combined gains in signal-to-noise ratio (SNR) and contrast mechanisms, it is now anticipated that imaging at this magnetic field will also impact clinical practice and that such a "clinical" scanner is inevitable. The thrust of this proposal therefore is to push these gains further, broadening the boundaries of MR research by providing the RF technology and knowhow to make the first human whole body imaging possible at 10.5 Tesla (~450 MHz proton frequency) and even higher to the current technology limits of 11.7T (500 MHz). 10.5 T represents a significant increase over the current, most commonly available ultrahigh field platform of 7 tesla. No such instruments currently exist in the world. The CMRR has the first 9.4T system capable of imaging human heads only, with a 65cm bore magnet and very narrow, asymmetric head gradients. Four such systems exist today. An 11.7 T, 68 cm bore (~500 MHz) "head only" system is planned for NIH intramural research. The rationale for continuing to advance the technology is based on the demonstration, largely coming from our laboratory, that (i) ultrahigh fields provide unique information that is not available at lower magnetic fields, (ii) such information can be obtained not only in the human brain but, with appropriate technological developments, in the human torso and extremities as well, and (iii) such information is useful both for basic biomedical and translational research as well as for clinical medicine. Specific demonstrations at 7T and 9.4T include:

- SNR gains in the human brain at such high magnetic fields (a concept that was questioned at the time) (28, 29),
- the feasibility of improved morphological imaging (28, 30),
- significantly improved fMRI contrast and accuracy (2-4, 8-11, 14, 31-35),
- higher resolution neurochemical spectroscopy (21-24),
- improved parallel imaging (36-38),
- feasibility of imaging in the human torso where the RF problems are the most difficult (39, 40).

If successful, this grant will first demonstrate the feasibility and advantages of a 10.5T system in the CMRR, a Biotechnology Research Center (BTRC) for high field MR research and a laboratory with appropriate

interdisciplinary expertise and infrastructure to maximally utilize it, and for an 11.7T system in a similarly resourced national laboratory in France, CEA Neurospin.

This proposal is the fifth in a highly productive series of grants that supports the core of the PI's research to advance the state-of-the-art in high field RF engineering and safety, from 3T and 4T to 10.5T and 11.7T over the time span 1998 through hopefully, 2015. The first grant (R01 CA076535 (2-10-1998 thru 1-31-2002)) advanced head imaging with transmit and receive birdcages and inductively coupled TEM coils at 3T and 4T to TEM transmit coils with local receive arrays, and to the door steps of multi-channel TEM (aka transmission line array) head coils at 3T to 7T (28, 41). Results and funding from this grant facilitated the bid for a DOD-ONDCP award to the Massachusetts General Hospital to launch their 7T program, and provided the coils, methods and safety data for acquiring the world's first 7T head images at the University of Minnesota, CMRR. The second and third grants in this line, EB 00895 (12-1-2002 thru 7-31-2009), achieved the first 4T whole body imaging (with B_1 shimming) (42), produced the first multi-channel (16x) transmitter for head imaging (29) and high-field body (43), numerous multi-channel transmit coils for 7T and 9.4T head imaging(28, 44-47), the first 9.4T head images (29), and the first examples of interactive, programmable B_1 shimming to make this possible. (48, 49) The fourth grant in this series EB 006835 (8-15-2007 thru 7-31-2011) continued improvements in 7T and 9.4T head imaging (39, 46, 50-52) and spear-headed the first whole body imaging at 7T.(43) This fourth grant, currently active until July 31 of this year, has provided many of the preliminary results from innovations to be developed and applied in the drive to 10.5T and 11.7T with the grant proposed. Not everything proposed for EB006835 was accomplished however, for a number of reasons. The five year proposal was funded for three, and the budget for three years was cut. The 11.7T magnet delivery schedule was planned for year five of the original proposal, and so was not available. So while 7T body imaging and 9.4T head imaging aims were largely accomplished, 11.7T research and development was deferred to this proposal. The new 10.5T system, not previously anticipated, now offers an additional in-house platform for whole-body MR at the highest fields. This grant is therefore critically needed to continue the progress on this highly productive, thirteen year project to advance the technology and methodology of high field human MR for the CMRR, for the CEA Neurospin, and for the rest of the international high field MR community.

B.2 Innovation

3T is the highest field strength used for clinical MRI. According to Frost and Sullivan, May 2010, sales of 3T units makeup the fastest growing MRI systems market with approximately 2000 installed worldwide. 7T is the highest field for "standard" factory supported systems with approximately 35 of these systems installed. Above this, four 9.4T systems exist, and one 11.7T, 68cm bore (head only) system is being installed at the NIH. Due primarily to technological and methodological shortcomings, most of the 7T and 9.4T systems are used for imaging only human heads or smaller lab animals. In particular, commercial RF head coils are not available for fields of 9.4T and higher, and commercial body coils are not available for 7T or above. While whole body 10.5T and 11.7T magnets for this study are being made available at the University of Minnesota and at the CEA in France, Figure 1, there are many additional technological and physical challenges to human imaging at these highest field strengths and accompanying Larmor resonance frequencies. The Larmor wavelengths in the human tissue dielectrics at 450 MHz (10.5T) and 500 MHz (11.7T) are on the order of 8cm and 7cm respectively in high water content tissues such as muscle and brain. By conventional methods and thinking, these wavelengths would preclude any possibility of achieving safe and successful human-scale imaging. RF interference patterns from conventional, uniform field volume coils would create severe RF field inhomogeneity in the anatomy. RF losses to the tissue conductor and the tissue dielectric would result in severe heating for conventional pulse protocols. Conventional RF coil and frontend circuits would be highly radiative (inefficient) with poor current and field control. New methods and technology being developed at the University of Minnesota may not only solve some of these problems, but may actually use the short wavelengths to new advantage. Examples of new innovations proposed for solving high field problems follow.

1.) World's highest field, whole-body magnets.

These magnets are uniquely innovative. While this proposal does not include magnet design, the fields generated by these magnets necessitate the many new innovations in the hardware and in the experiment protocols of this proposal.

2.) New methods of modeling the human body at new, highest frequencies.

See Figure 2. The success of coil systems' design and operation will depend heavily on new approaches to modeling. Modeling RF field propagation and losses of multiple wavelengths in human anatomy is required for safe and successful imaging. Safety can no longer rely on course calculations of E fields and SAR alone. Numerical predictions of heating (ΔT) and temperature contours (T) must be included. These thermal models must be accurate and precise to 0.2°C. The accuracy and precision of the SEMCAD X FDTD solver (Speag, Zurich, CH) (53) will be enhanced by our improved bioheat equation (54), and validated in first-of, whole body experiments with porcine models. (55)

3.) Porcine Anatomy Atlas.

In order to validate thermal models with direct measurements, a porcine anatomy atlas will be created. Examples of segmented anatomy derived from MRI of a pig's head are shown in Figure 3. This unique work must be done for the whole porcine body as well. The World Health Organization recommends this model for investigations of RF dosimetry, heating, and heat stress. (56)

4.) New head coil systems. Head coils don't exist for 10.5T or 11.7T imaging. Existing approaches can't be used for successfully imaging the whole head at these fields. Significant innovation will be required for a successful design. The coil systems proposed will include short, efficient, "3D", shielded coil element arrays, using linear elements for transmit, loop elements, decoupled by orthogonality will be used for receive elements. The elements will be electronically tuned and matched. On-coil decoupling preamps, power amplifiers, and transmit/receive (TR) switches are design goals. As many as 32 transmit channels and 64 receive channels will be distributed in x, y, and z for "3D" B1 shimming. Figure 4 includes pictures of a lower frequency prototype with an early 9.4T image

Figure 1.
World's highest field magnets.



Courtesy: Magnex Scientific Ltd., Yarnton, UK

Courtesy: Vedrine (Ifu), Lethimonnier(DSV), Wiggins (NeuroSpin)

	10.5 T CMRR	11.75 T NeuroSpin, (Saclay, FR)
Field / diameter	10.5T / 880mm	11.75T / 900mm
Magnet Manufacturer	Agilent	Iseult, CEA NeuroSpin,
Temporal stability	0.03 ppm/hour	0.05 ppm/hour
Spatial homogeneity	< 0.07 ppm 250mm dsv	< 0.05 ppm within 220mm dsv
Current		1483 Amps
Stored Energy	280 MJ	338 MJ
Conductor	NbTi (1433 km)	NbTi (56 tons)
Temperature	3 K	1.8 K
Size	4.1 x 3.2 m	5.0 x 5.2m
Weight	110 Tons	136 Tons
Delivery	October, 2011	October, 2013 (At field)

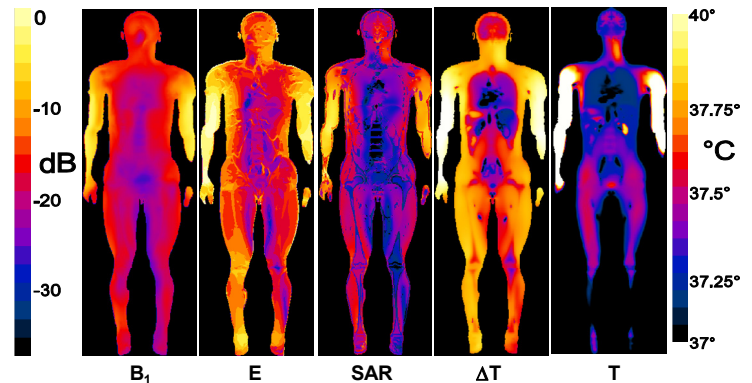


Figure 2. Calculated relative RF magnetic field (B_1), RF electric field (E), specific absorption rate (SAR), temperature change (ΔT), all on log scale (dB), and absolute temperature (T, °C) for 133 W, 300 MHz RF input into a 72 kg human body from a 60 cm i.d. x 1 m long TEM body coil with 33cm elements centered on the thorax.

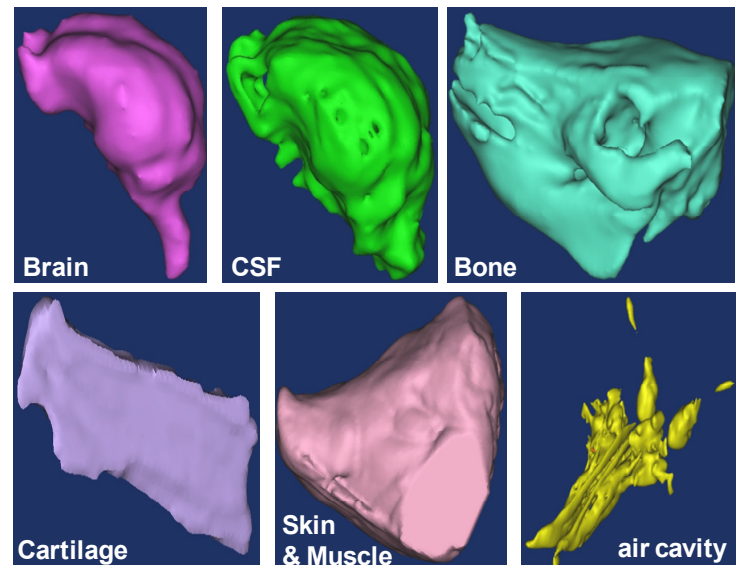


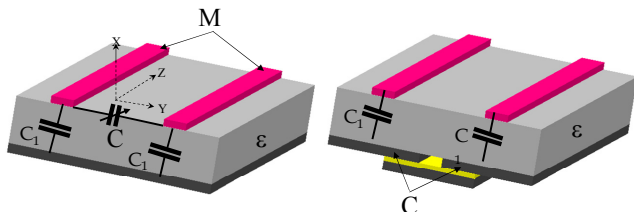
Figure 3. A segmented porcine head model developed in-house.

zoomed for detail. (29) The coil includes practical features such as front to back view port channel, and a compact diameter (32cm) that fits into a head gradient coil set.

5.) New body coil systems. Other than at the CMRR, a whole body coil does not even exist for 7T. See Figure 7. Proposed here are 10.5T and 11.7T full, 32 channel body coils together with 32 and 64 channel receive arrays. Similar to the head coil above, the proposed body coil will incorporate on-coil power amps, preamps, TR switches and feedback driven, auto-tuning circuitry.

6.) Novel and necessary coil element decoupling.

The 32 channel TEM elements must be decoupled to 20dB or better for best parallel imaging and B_1 shimming performance. A new method for cancelling mutual inductance M between elements with shield capacitance, C , in Figure 6 (right) will limit losses and field perturbations associated with conventional capacitive bridging as shown in Figure 6 (left). (43, 57)



$$M = \frac{\phi_{21}}{I_1} = \frac{\mu_0}{4\pi} \iiint_{xz} \left[\iiint_{y_0=0} J \left[\frac{j\beta}{r'} + \frac{1}{r'^2} \right] e^{-j\beta r'} \frac{x-x_0}{r'} dy_0 dz_0 \right] dx dz$$

Figure 6. Decoupling coil elements by cancelling mutual inductance, M , using the usual practice (left) compared to the proposed method using shield capacitance (right).

7.) On-coil power amplifiers are a new innovation.

Due to cabling issues, power loss, and prohibitive expense of high-power amplifiers, it's difficult to imagine a 32 element 3D coil without local, on-coil (or proximate) power amplifiers. To test feasibility of this concept, class AB linear power amplifiers were tested in the magnet with a single amplifier driving a single TEM element to image a phantom. It works. Proposed is a more compact, significantly more efficient (without finned heat sinks) class E nonlinear power amplifier that can be pre-compensated for linear output and mounted right on a coil element. This innovation alone will revolutionize coil and MR system design.

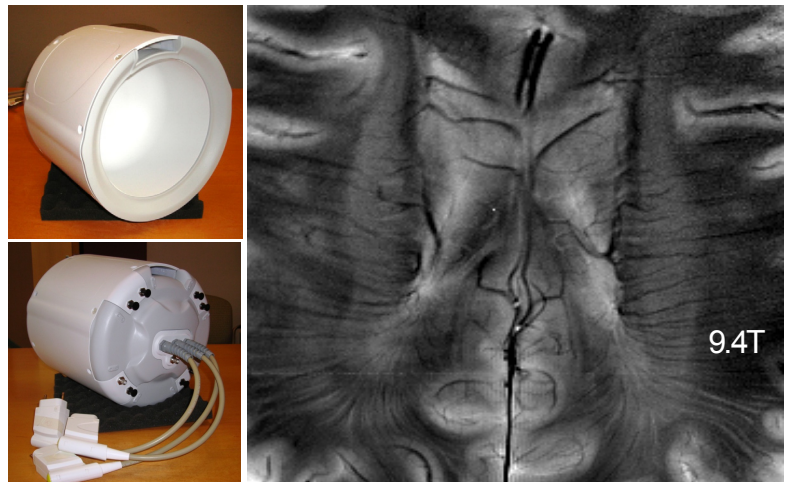


Figure 4. High frequency head coils consisting of multi-channel TEM transmit coils with multi-channel receive arrays. Detail in a 9.4T T_2^* weighted, zoomed FLASH image of a human brain is shown.

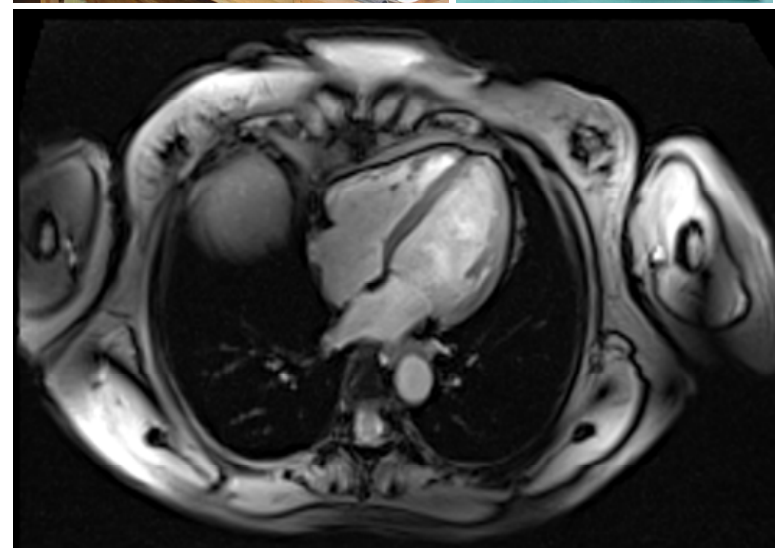


Figure 5. A 16 channel, 7T body coil, half of a 32 channel receiver, and a single frame of a B_1 and B_0 shimmed, cardiac cine acquired with the 16 channel transmit, 32 channel receive system.

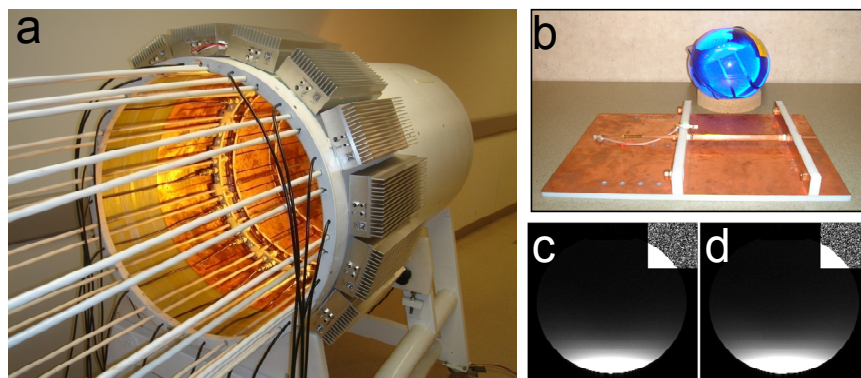


Figure 7. Local power amplifiers mounted on multi-channel, 7T body coil (a). Single TEM channel element (b) used to acquire phantom image with local amplifier (c) and with remote amplifier (d). Image (c) was acquired with $\frac{1}{2}$ power of image (d).

8.) Automatic tuning and matching is also highly innovative and needed.

A high frequency, multi-channel transmit coil must be tuned and matched per subject. Currently in the lab this is done manually, one element at a time. Note in Figure 7a the 16 tuning and 16 matching stems that must each be adjusted for each scan. Even if the applications scientist would not mind using a major part of her experiment time tuning and matching multiple coil elements, the coils proposed with double the element count and inaccessible elements would make such manual adjustments impossible. The RF signal feedback driven, PIN diode switched, capacitance matrices for tuning and matching each coil element electronically, automatically with algorithm control, Figure 8, is therefore an innovation needed for the coils proposed, and for all practical multi-channel, transmit coils.

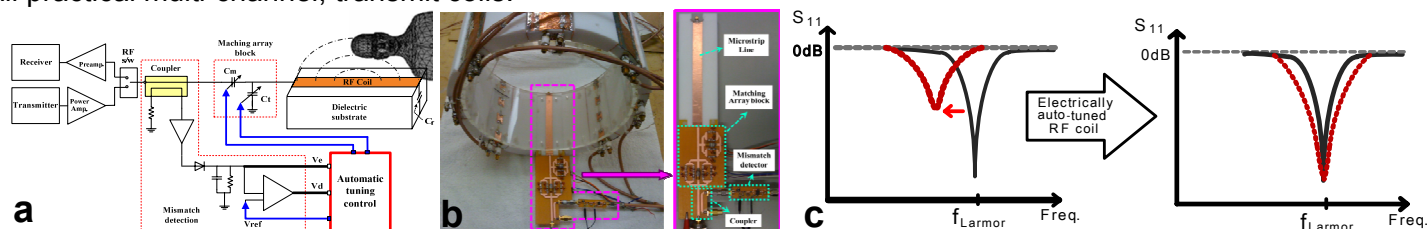


Figure 8. Electronic auto-tuning. Every channel in a multi-channel coil must be electronically tuned and matched per subject for best results. A feedback algorithm driven, PIN switched capacitance matrix adjusts frequency tune and impedance match per element, in-situ. Diagram 8a details the circuit, b shows a prototypical implementation of the circuit into a single coil element, and c shows a modeled result.

9.) On-coil transceiver

Extending from Figure 7 technology above, a high performance, low cost solution (integrated power modulator units) to the costly and cumbersome parallel transmitters and receivers now driving multi-channel coils will be designed, built and implemented in the new head and body coils of this proposal. Combined with the preamplifiers in the coil, a high speed parallel transceiver will be developed and implemented for automated B_1 shimming Transmit SENSE, and other “on the fly” applications at 10.5T and higher. The 66 μ s command cycle of first generation transceivers is sufficient for controlling phase and gain settings for interactive RF shimming. But these are too slow for many other important applications. The new system proposed will reduce this time delay to a sub-microsecond control cycle to facilitate Transmit SENSE, automated shimming and other high speed applications requiring on-the-fly waveform modulation and feedback control. The broadband power amplifiers and other system components also allow for simultaneous or interleaved multi-nuclear applications, swept frequency methods, and other frequency dependent protocols.

At the heart of the second generation parallel transceiver proposed is a transmitter module consisting of a single chip modulator, and a single Field Effect Transistor (FET) power amp. The compactness of this unit (approximately 1cm x 2cm x 3cm) will make it possible to integrate this unit with its dedicated coil element. Together with a similarly compact PIN diode protected preamp, this second generation parallel transceiver will be integrated at the probe head (coil) for maximum RF speed, performance and flexibility. A coil with local phase, gain, frequency, temporal, and spatial (per element) control will bring a true paradigm shift to the concept of an RF coil and equally to a new family of RF excitation sequences to take advantage of this new technology.

To build the new device, an adjustable integrated circuit will be designed that allows for frequency shifting over 100 kHz of bandwidth, phase shifting over 360 degrees, and amplitude adjustment over 30dB. The circuit architecture will consist of the blocks shown above, Figure 9. The incoming signal will be amplified to a known output value through an automatic gain control (AGC) circuit to maintain optimal operating conditions for the mixer. This signal will be mixed with a low frequency signal to adjust the input signal around the center frequency. The low frequency signal will be produced by a voltage-controlled oscillator (VCO) controlled through the frequency adjustment line. The output of the mixer will then be supplied to the phase adjustment circuitry. The phase of the signal will be modified according to the phase control signal from zero degrees to 360 degrees through capacitors that are switched into the system. Last of all, the signals' amplitude will be adjusted as required by the system, taking into account the fixed input amplitude supplied via the AGC.

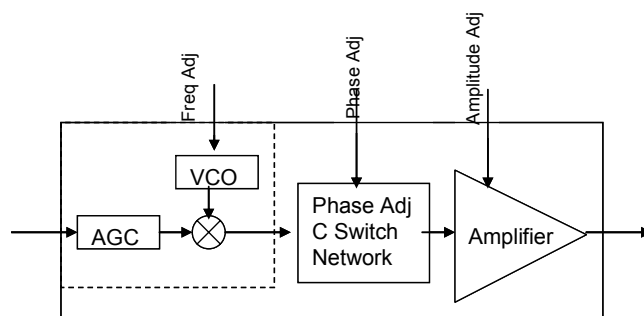


Figure 9. RF transmit signal phase and magnitude (gain) modulator with power FET (amp).

Due to the need for linear, high voltage signals, a bipolar junction transistor (BJT) process such as IBM's 0.35 μ m SiGe best suits the needs of the project. The first pass of this design will take approximately five months of design effort followed by a month of layout and two weeks of re-simulation. The design will be verified in simulation against the system specifications that will be developed first. From the specifications, a system architecture will be decided upon and implemented. Each circuit block will be designed and simulated to the specifications of the architecture and then combined into the full architecture for system simulation. From here, the circuits will be laid out, checked, and extracted. Using the extracted decks, the system will be re-simulated to ensure that parasitics of the chip are not affecting the system performance. These simulations will be performed with Analog Artist, Spectre, and Spectre RF; layout will be performed with Vituoso XL; and checking will be done with the appropriate checking decks for the process.

B.3 Approach

A general engineering approach toward reaching design goals for safe and successful coil systems and their operational protocols will be followed. This approach consists of 1. specification and design, 2. construction, 3. test and evaluation. These steps often require iterations of each step before the design goals are met. The Specific Aims for head and body coil development generally follow this engineering approach.

Aim 1. Head Imaging Coil, 10.5T to 11.7T.

1. **Specification and Design:** Head coils for 10.5T and 11.7T will be built in years 2 and 4 respectively to meet the following criteria. Physical: The i.d. must be 25cm to snugly fit most human heads (and noses), together with a foam head cup and ear protection. The o.d. will be constrained to 33cm to fit on top of the patient table, but within optional head gradients. An optical view port will be incorporated into the roof of the coil to permit forward or rear projection screen viewing by means of a configurable mirror. See Figures 4,11a. The coil shall be packaged and connectorized to meet IEC standards. Based on modeling and extrapolation from experience at lower fields, reasonable performance goals are : $B_1 = 0.23 \text{ uT/W}^{1/2}$ peak; 15 cm dsv, B_1 shimmed to 80% homogeneity with efficiency = $0.1 \text{ uT/W}^{1/2}$; iSNR $>165/\text{uL}$ in head center; 1.2 mean g factor for a 4x3 2D reduction factor; decoupling 18dB nominal. SAR = 0.4 W/kg/W.

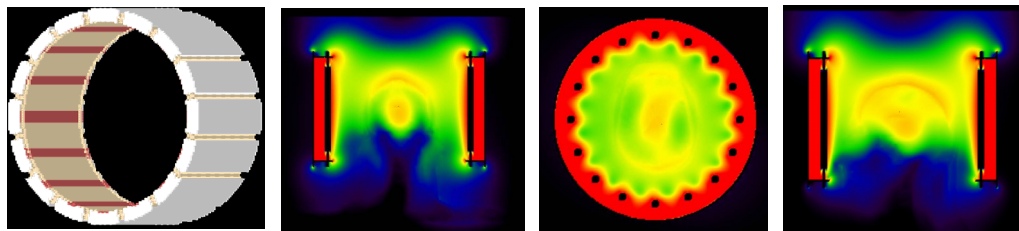


Figure 10. 9.4T Predictions of non-uniformities in a head with a 16 element, homogeneous CP coil. Each color represents a 20 dB, B_1 field contour. This coil and current drive scheme are clearly suboptimal.

2. **Construction:** To meet these performance specifications, a head coil consisting a thirty two channel receiver nested with a thirty channel TEM TR coil will be built, for a combined total of thirty transmit channels and 63 receive channels. Simulations suggest that this configuration will produce good depth of B₁ coverage in the head. Thirty, 8 cm TEM transmit and receive elements will be arrayed in a 2x15 configuration per Figure 11c, leaving room for view channel over the face. The 2x15 array will better cover the whole head together with x.y.z. "3D" B₁ shimming, to correct the B₁ field nonuniformities shown in Figure 10. Short, 8cm elements will

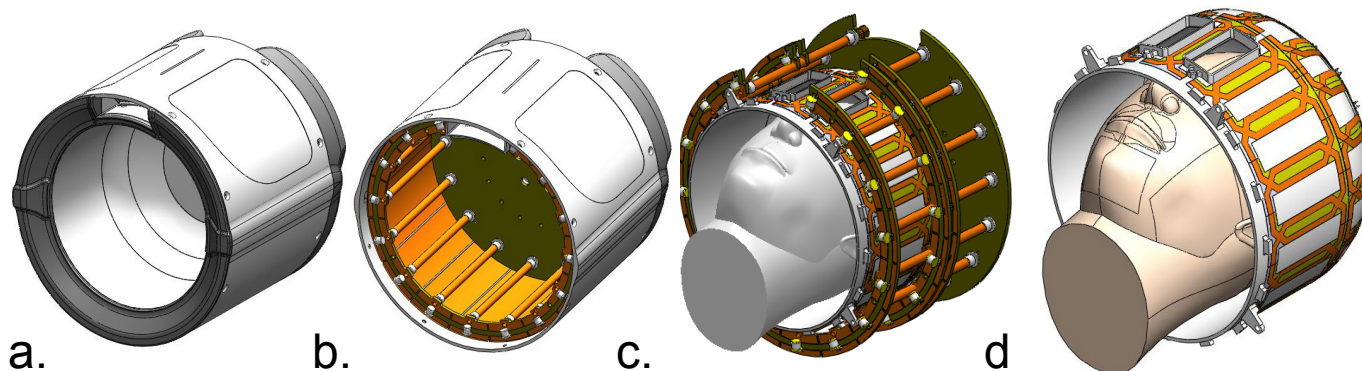


Figure 11. High frequency, "3D" head coil system disassembled to show the compact package with view port (a), the slotted, capacitive shield (b), 32 auto-tuned TEM transmit/receive elements in x,y,z, (c), and the 32 channel receive elements (d).

also be less radiative and more efficient at 450 – 500 MHz. The shielded TEM elements as shown un-split in Figure 11b will be decoupled by the innovative method described in Figure 6 to an adequate 18 dB decoupling. Thirty-two receiver loops will be arrayed in a 2x16 configuration per Figure 11d. The loop receive elements will be centered with the linear transmit/receive TEM elements for maximum orthogonal field decoupling between the two circuits as shown in Figure 11c. Orthogonal decoupling, decoupling preamps, and additional capacitive bridging, if necessary, will ensure 18 dB decoupling between the loop receiver array and the TEM transceive array. The TEM array will be electronically tuned and matched per Figure 8, and ultimately driven by thirty local, on-coil amplifiers described in Figure 7. Ultimately, the on-coil transceiver will move most of the RF spectrometer onto the coil itself, significantly saving performance, cost, bulk and complexity of the front end of the console.

3.) Test and Evaluation

Before a coil or array is put into service, it is rigorously tested, evaluated, and characterized both on the bench and in the magnet. Coil resonance, Q, and isolation, in both the loaded and unloaded condition as well as dynamic detuning are verified on the bench. In the magnet, coil coupling, image homogeneity, transmit efficiency, and SNR are characterized. Unfortunately, for high-field coils these conventional metrics are often insufficient to completely characterize and describe the transmit degrees of freedom, spatially varying characteristics of the coils, and the potential synergy of RF coil fields and imaging methodology. More characterization is needed. The noise covariance matrix (58), Figure 12a of the loaded array is computed from the collected noise data. B₁⁺ shimming calibration data is then acquired. (48) Individual receiver data is used to calculate receiver sensitivity maps and geometry-factor maps, Figure 12b.(58) The magnitude of the B₁⁺ is mapped with two fully-relaxed gradient echo images collected with excitations nominally set to 60° and 120° (double angle method), Figure 12c. (59) Additionally, the 60° excitation gradient echo image is carefully post-processed so that the result is in SNR units.(60) Using the B₁ map, the SNR image, and

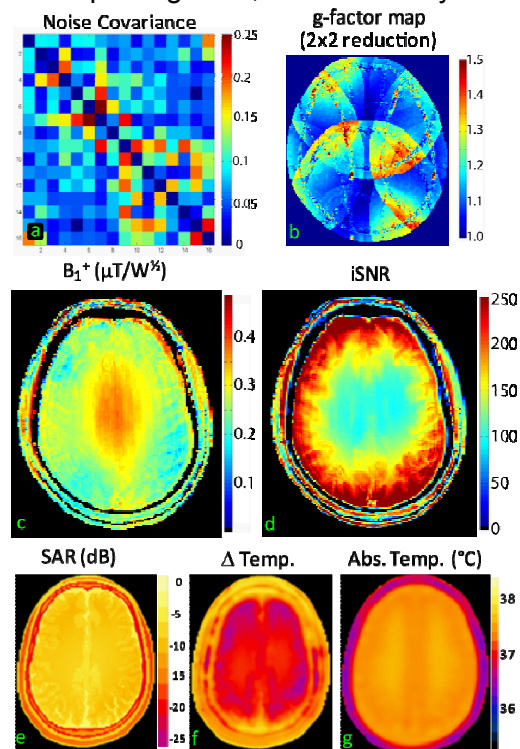


Figure 12. Example coil characterization data of a custom 7T TEM transmit/16 loop receive head coil.

acquisition parameters, the SNR image is converted into intrinsic SNR units which describes receiver performance independent of transmit performance, Figure 12d.(45) By combining the above data, single-channel transmit field maps can be synthesized to predict the transmit efficiency for any B_1^+ shim. The transmit efficiency verses transmit homogeneity can then be calculated for a region and reported for the constraints of 90%, 80%, and 70% transmit homogeneity. Electromagnetic modeling is used to predict the SAR, Figure 12e, change in temperature, Figure 12f, and absolute temperature, Figure 12g. Imaging five volunteers for each coil would be sufficient to report a coil's characteristics statistically. However, optimizing a coil prototype is an iterative process requiring ten additional volunteers per coil. This coil characterization provides the information needed to predict parallel acceleration performance, transmit efficiency, transmit homogeneity, and the SNR for an arbitrary imaging sequence. Accordingly, progress toward reaching the stated performance goals can be checked and validated. Furthermore, these results are reported in units that can be compared across systems and field strengths.

Aim 2. Body Imaging Coils, 10.5T to 11.7T.

1.) **Specification and Design:** A 32 channel (2x16) TR whole body coil combined with a 32 channel receiver is proposed. Based on the bore size of the new Siemens SC72 gradients for the new 10.5T and 11.7T magnets, the o.d. of the new body coil must be slightly less than 72cm. Extrapolating from experience with similar design at 7T (Figure 5), we can set minimum performance specifications to be: $B_1 = 0.1 \mu\text{T}/\text{W}^{1/2}$ peak; $B_1 = 0.05 \mu\text{T}/\text{W}^{1/2}$ for B_1 shimmed to 80% homogeneity over a 15cm dsv; $i\text{SNR} > 70/\mu\text{L}$ in central structures like the prostate. Central slice g-factor = 1.2 for a 6 x 3 2D reduction factor. Coil element decoupling 18 dB nominal. SAR = 0.5 W/kg/W.

2.) **Construction:** The 32 channel TEM transmit and receive (TR) coil structure will consist of a double sided, slotted cavity lining the inside of a fiberglass bore tube of dimensions 71.5cm x 120cm. 32, 15 cm long TEM elements will be configured in a 2x16 array. These elements will be secured to the o.d. of a second, 5mm wall thickness fiberglass tube of 65cm o.d. x 120 cm length. Initially available to drive this transceive body coil (and the head coil) are 32, 1 kW power amplifiers at the CMRR. However, the plan is to build on-coil 1 kW power amplifiers, and then on-coil power modulators described with Figures 7 and 9 above. These will be added to the Neurospin coil as well. Each of the 32 elements will be auto-tuned as described in Figure 8. The receiver coil planned will be a close fitting pair of 16 element "breast plates" for a combined 32 channel receiver. See Figures 5 and 13. The full RF body coil system will include 32 transmit channels and 64 receiver channels for best B_1 FOV coverage, 3D B_1 shimming capability, and parallel transmit and receive performance.

3.) **Test and Evaluation:**

T&E will proceed as described for the head coils in Specific Aim 1. While a similar basic coil system (though far less sophisticated) has been demonstrated to be successful at 7T, radiative losses from the coil circuits and tissue losses from the human load will increase significantly at 10.5T and 11.7T. An effort to anticipate these losses was incorporated into the minimum performance goals, together with performance specifications required for at least, FLASH imaging protocols. However, if the performance of the whole body coil does fall short of its design goals, an alternative approach will be considered.

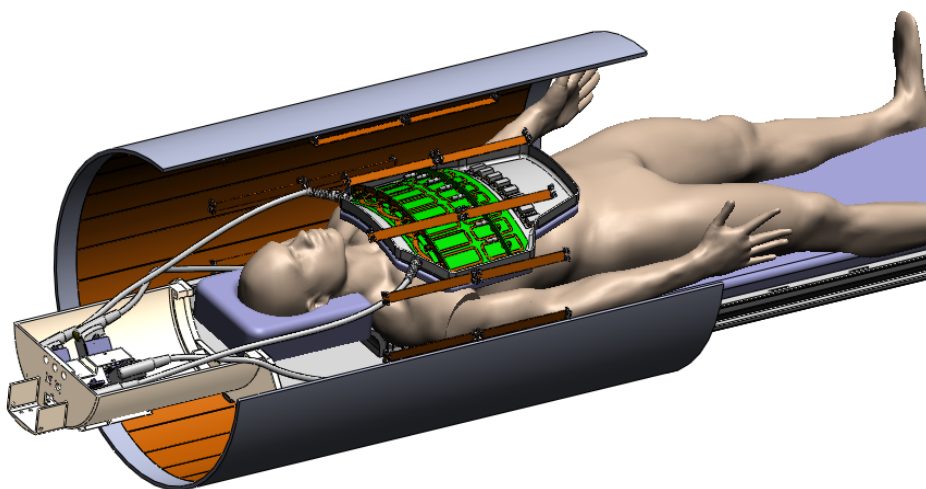


Figure 13. High frequency "3D" body coil system comprised of 32 channel transmit and receive elements and a 32-channel loop array within.

4.) Alternative Design

Pictured in Figure 14 is an alternative, proven approach to body imaging. (39, 49, 61) To conserve RF power, this approach applies transmit coil elements arrayed close (5cm) to the body. Sandwiched between the 16 transmit elements (8 top, 8 bottom) and the body are receiver arrays which will be configured as 2x8 top and 2x8 bottom for a total of 32 channels. While the proposed PIN switched capacitance matrix (Figure 8) could be deployed with this design, an alternative approach to auto-tuning and matching is shown. This approach makes use of piezo motors to electromechanically drive tuning and matching of the TEM transmit elements. (62-64)

Aim 3. RF Safety 10.5T to 11.7T.

The primary purpose of this Aim is to assure human safety in for the first human studies at these unprecedented field strengths. Local SAR and temperature contours will be numerically predicted using digitized porcine and human models for heads and bodies. Systemic and local temperature predictions will be validated in direct measurements in anesthetized pigs, in vivo. Measured temperature in pigs will be correlated to measured SAR using the same coils, amplifiers, and protocols proposed herein for human use. In addition to publishing the data acquired from these studies, it will be submitted to the FDA and to our IRB in annual progress reports.

1.) Modeling and Design

SAR and temperature will be modeled in digital porcine models at 450-500 MHz in order to create a porcine model that can be directly validated by fluoptic measurements. For human sized RF coils at 450 and 500 MHz, phantoms adjusted to physiologic conductivity and permittivity are only useful for loading the MR system to verify proper system circuit and control functions. By our experience, even the best phantoms (mimicking physiological electrical properties, geometry, tissue segmentation, etc.) at these frequencies and dimensions are not very accurate or precise when predicting in vivo safety data. For this purpose, we have through many years of experience, come to rely on porcine models to predict heating of tissues exposed to RF energy. In addition to the most accurate electrical properties (conductivity, permittivity, permeability) the anesthetized pig model supplies the thermodynamic properties (specific heat, perfusion, metabolic heating and thermoregulatory reflexes e.g. heart rate, vasodilation, etc.) necessary to truly investigate RF heating in a living system of approximate human size, mass, and temperature. NMR imaging parameters for a live pig are also more similar to human measurements. Also, farm pigs are desirable for their availability, inexpensive cost, and

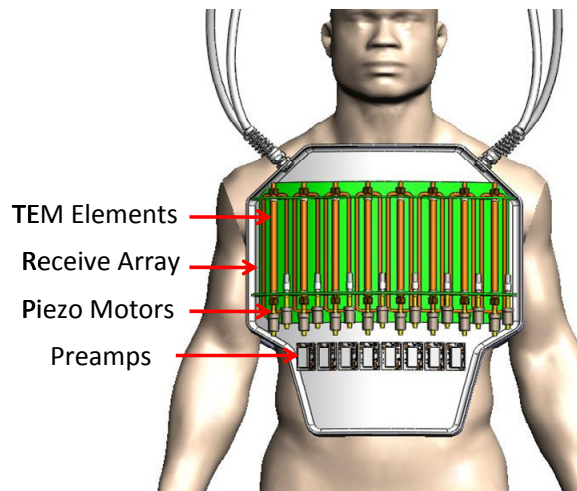


Figure 14. High frequency torso array comprised of 16 channel transmit and 16 channel receive (eight channels top, eight channels bottom).

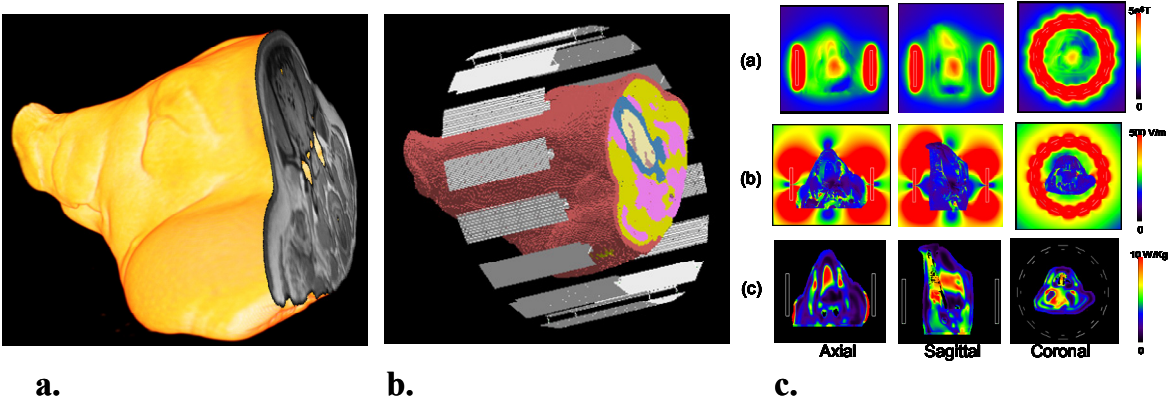


Figure 15. In the model above, 15a shows a pig head rendered from MR images. Figure 15b shows a FDTC model of the pig head with segmented anatomy in a coil. Figure 15c shows the center slice B1 field (a), E field (b) and SAR (c) in 3D.

unlike human subjects, they can be measured directly by invasive means.

Direct temperature measurements from the tissues of live pigs can be used to validate and calibrate numerical models which can then be used to predict and understand RF heating and SAR. To make this possible, digital models of the pig (whole body this time) must first be created by the approach demonstrated in Figure 15 below. In 15a, a pig's head was imaged with a 3D multi-slice protocol. From this 3D image data set, the tissue boundaries were edge detected and the tissues segmented as in 15b. Each tissue segment was then assigned table values for conductivity and permittivity (dielectric constant). B_1 field, E field, and SAR could then be numerically calculated for a given coil design, placement, and excitation. The SAR (power loss density) can then be equated to temperature through the Pennes' Bioheat Equation or better, or own generalized bioheat transfer equation.(54) Our models and methods will then be calibrated, tested, and validated with additional pig studies.

RF heating (the actual safety issue) will be calculated and measured in porcine models of adult human weight to identify the RF power level limit that can be safely transmitted from the head and body transmit coils being developed for this grant. The FDA has specified guidelines for RF energy dosimetry to the human body in two ways: 1) Average and local specific absorption rates (SAR) as discussed above, or 2) RF power deposition must not create a core temperature increase in excess of 1 °C or localized heating to greater than 38°C in the head, 39°C in the torso or 40°C in the extremities. Equating the power loss density to temperature through the bioheat equation, temperature contours will be calculated for 3D head and body models.(65) Contours will be calculated for the human head and body for each RF head and body transmit coil used. The result will be coronal, axial, and sagittal, temperature maps for each coil system, and for each frequency 450 and 500 MHz.

2.) Testing and Evaluation

By measuring RF power vs. temperature in porcine models by fluoptic thermometry, our goal is to correlate RF power to RF heating measurements in live pigs in order to directly identify FDA temperature guideline limits. RF coils used for these measurements will be characterized in terms of °C/W/kg.

It is prudent to validate temperature models by direct temperature measurement. Why? Because the thermal criteria most directly influence the underlying safety issues (localized thermal tissue damage, systemic stress, etc). Also, local temperature can be directly measured in the porcine model, and temperature contours are more extreme due to shorter wavelength losses in tissue at higher frequencies. Temperature will be measured on the coronal, axial, and sagittal planes modeled, rectally, and also adjacent to receiver coils placed on the porcine model within the head and body coils. In this way any power coupled to receiver loops will be monitored for local heating, in addition to the measured core heating. Figure 16 illustrates the technique of fiber optic probe placement (guided by porcine digital model of Figure 15) in a perfused porcine model, within a coil field. This study will use the same arrangement in the head and body of the pig model.

To secure a minimum of N=5 measurements per study, five, 70 kg farm pigs will be used to test each coil system, at the rate of one coil per year to assure RF safety of the coil before human studies with the coil begin. A total of twenty pigs will be required for the four-coil, four-year study. To most accurately simulate the RF portion of the NMR experiment, anesthetized pigs will be placed on a patient table bridge, inside the head or body coil. RF power will be set to the SAR guideline limit for humans. Temperature vs. time will be measured for multiple locations inside the pig model until the temperature reaches steady state, or until the FDA temperature limit is reached locally or globally. The head or torso will be instrumented with seven temperature probes from the eight channel Luxtron thermometer. The eighth probe will remain in a thermometer referenced control cell (water bath) outside the coil. For transmit power input from the coil, temperature will be measured in the anesthetized pig's head or chest. This study seeks to identify the location and magnitude of "hot spots", then to correlate the RF coil input power with hard to detect, RF coil specific heating patterns and limits in tissues.

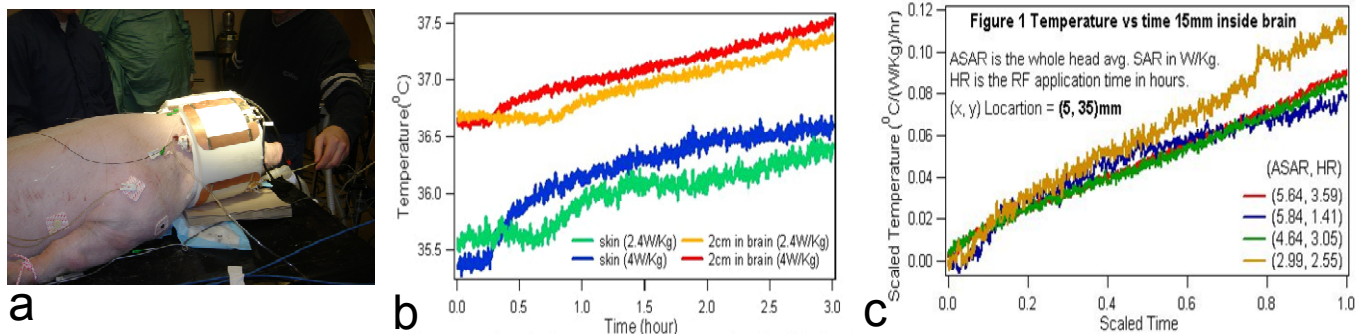


Figure 16. Figure 16a shows a laboratory set up for direct measurement RF protocol induced heating. Figure 16b plots temperature vs. time measurements as obtained from fluoro optic probes placed at various and model guided positions in the head and brain. Each trace registers a different probe position in the tissue. In this experiment, SAR will be correlated to heating for coil applications, using the porcine model for human studies planned. Finally, plot 16c shows a “thermal characteristic” of the head coil shown in 16a.

The following data grid (Table 1) will be completed two times for each of 20 pigs (5/yr.), first for an In vivo experiment with anaesthetized pigs, then for another experiment immediately after sacrifice to determine the worst case (non-perfused) conditions. The measurement grid below will be completed for body and for head at 450 MHz and 500 MHz.

Table 1.

Temperature, °C vs. time will be recorded for the following parametric permutations:

Coil	Power probe	1	2	3	4	5	6	core	cal	h.r.	B ₁
10.5T Head	@maxSAR	?	?	?	?	?	?	?	?	?	?
10.5T Body	@maxSAR	?	?	?	?	?	?	?	?	?	?
11.7T Head	@maxSAR	?	?	?	?	?	?	?	?	?	?
11.7T Body	@maxSAR	?	?	?	?	?	?	?	?	?	?

A more detailed explanation of the methods used to fill the data grid follows. Fluoro optic probes from a Luxtron 3000 unit will be inserted via an 18 gage hypodermic needle, into the drilled head or chest wall muscle. A linear probe with transducers 1-4 spaced at 1 cm intervals will be positioned in the brain, or subcutaneous fat and intercostal muscle, centered beneath the receiver coil, to a depth of 0 to 4 cm. Two more single transducer probes will be inserted into the scalp, or chest wall immediately beneath the receiver coil elements to measure local heating adjacent to the coil conductors. A seventh transducer will be inserted rectally to monitor the core temperature of the animal, outside the body coil. The eighth remaining probe is dedicated to a water calibration bath apart from the animal measurements. The heart rate, h.r. will be monitored. B₁ for each power setting and frequency will be measured at the head or chest wall with a field probe, after the animal is sacrificed. The coil input power P will be determined using a four port directional coupler and a power meter. The line losses to the coil will be calibrated, as will any reflected power. Past experience indicates that each heating study from resting state to guideline limit heating, and back to resting state takes about 4 hours. Two studies per pig will require a minimum of 8 hours.

We can know for a given coil coupled to a given tissue mass with a given RF power input, what the temperature vs. time chart will look like. This is very useful information for determining the safety of experiments a priori. Such data will be determined for the coils before they are used in human experiments. Much of our IRB and IDE record is supported by our combined approach of modeling, measurement, and cumulative experience with both. The predicted sources of error from the experiments above will be due to the anesthetically suppressed thermoregulatory reflexes of the pigs. Resulting errors will be conservative (safe), predicting slightly more heating than will occur in non-anaesthetized, healthy humans. The body of data will tabulate a priori information correlating RF power input to maximum local temperature contours for the different coil combinations, applications, and frequencies. Also in the data are the heating rates for these parametric variations.

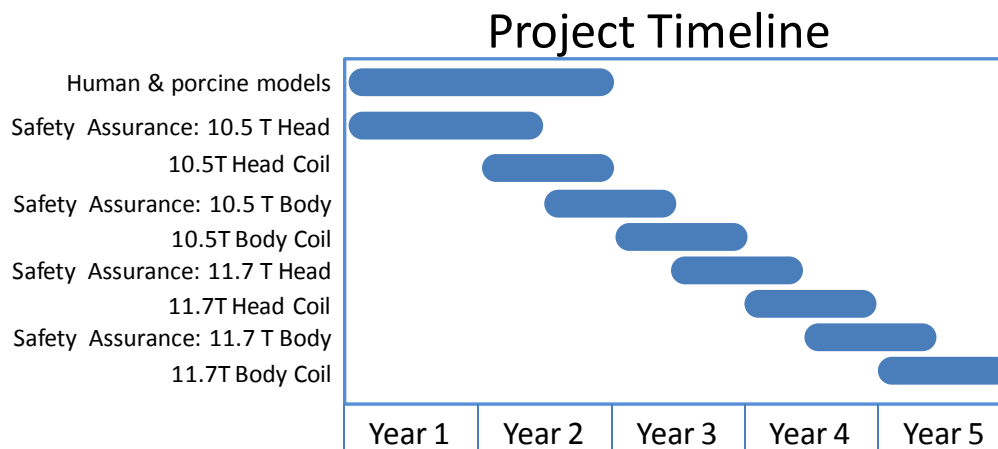
3. Safety Assurance Implementation

To assure human safety in the planned investigations, system power monitors will be set using either 1.) FDA SAR guideline limits for head or body, or 2.) measured SAR values correlated to FDA temperature guideline limits, whichever is the lower value. In this manner, we can be better assured that we are compliant and safe.

RF power needs to be monitored per channel in multi-channel transceiver coils. To monitor forward and reverse power for a 32 element coil, a 64 channel RF power meter is required. Such a meter does not exist from a commercial source. Therefore this instrument is being built in-house with other support. It will be built and integrated with a failsafe feedback loop into each MR system used in this investigation. This equipment will be in place and tested before human subjects are imaged. A priori information determined from the SAR and temperature modeling and measurement components of this proposal will be used to establish and set RF power limits, per coil, load, and power setting for a given experiment. Forward and reverse power will be monitored per channel. Each channel will be independently limited. Additionally power will be integrated for all channels. In this way, both local and global power will be monitored. When any preset limit is exceeded on single or multiple elements, a redundant failsafe will both blank RF power input to the parallel transceiver, and will power off each power amplifier of the parallel transceiver. These practices will be installed prior to human use.

Project Time Line

The timeline for this project will generally follow the outline of the Aims below, advancing with the field strength of the magnet, but with safety studies and implementation coming early. To move the field of human MRI into the “Deca-Tesla / centimeter band” range, the proposed project is necessarily ambitious in scope, and highly multi-disciplinary. Parallel progress is required on multiple fronts to move this field forward. There are few obvious “starting points” as much of this work as evidenced by Preliminary Results and Appendices is already underway. There are few obvious “end points” as development of the full potential of 10.5T and 11.7T MRI will require significantly more effort and resources than proposed herein. In time and human resources, the proposal seeks only to defray the much larger costs of moving high field MRI ahead to the next tier. This proposal also looks to leverage the significant investment already made by the NIH, the University of Minnesota, and CEA NeuroSpin to launch the first whole body systems higher than ten tesla. Most importantly, this project strives to introduce new and powerful MRI technology, methodology, and applications for the benefit of biomedical science. A twelve page proposal necessarily limits the detail into which an ambitious proposal can delve. It is therefore hoped that those reviewing will appreciate the experience and productivity of the team proposing this work.



Progress Report Publications List

The publication productivity stemming in whole or in part from this grant is extensive in count and dimension. The current grant, EB 006835 and its pedigree of predecessors have supported all RF coils and RF safety protocols for a large, productive research lab, the Center for Magnetic Resonance Research (CMRR). All of the papers, abstracts, patents, books, and chapters listed have directly benefitted from custom RF coils, RF safety modeling, measurement, monitoring, and other support from this grant and its investigators, staff and students. The list below, as extensive as it is, does not reflect the entirety of this grant's impact on the field.

1. Peer Reviewed Journal Publications

1. Adriany G, Van de Moortele PF, Ritter J, Moeller S, Auerbach EJ, Akgun C, Snyder CJ, Vaughan T, Ugurbil K. A geometrically adjustable 16-channel transmit/receive transmission line array for improved RF efficiency and parallel imaging performance at 7 Tesla. *Magn Reson Med.* 2008;59(3):590-7.
2. Marjanska M, Waks M, Snyder CJ, Vaughan JT. Multinuclear NMR investigation of probe construction materials at 9.4T. *Magn Reson Med.* 2008;59(4):936-8.
3. Metzger GJ, Snyder C, Akgun C, Vaughan T, Ugurbil K, Van de Moortele PF. Local B1+ shimming for prostate imaging with transceiver arrays at 7T based on subject-dependent transmit phase measurements. *Magn Reson Med.* 2008;59(2):396-409.
4. Shrivastava D, Hanson T, Schlentz R, Gallagher W, Snyder C, DelaBarre L, Prakash S, Iazzo P, Vaughan JT. Radiofrequency heating at 9.4T: In vivo temperature measurement results in swine. *Magnetic Resonance in Medicine.* 2008;59(1):73-8. PMID: PMC2754718.
5. Wang Z, Lin JC, Vaughan JT, Collins CM. Consideration of physiological response in numerical models of temperature during MRI of the human head. *J Magn Reson Imaging.* 2008;28(5):1303-8. PMID: PMC2597208.
6. Collins CM. Numerical field calculations considering the human subject for engineering and safety assurance in MRI. *NMR Biomed.* 2009;22(9):919-26. PMID: 2836719.
7. Shrivastava D, Hanson T, Kulesa J, DelaBarre L, Iazzo P, Vaughan JT. Radio frequency heating at 9.4T (400.2 MHz): in vivo thermoregulatory temperature response in swine. *Magn Reson Med.* 2009;62(4):888-95. PMID: PMC2782895.
8. Shrivastava D, Vaughan JT. A Generic Bioheat Transfer Thermal Model for a Perfused Tissue. *Journal of Biomechanical Engineering.* 2009;131(7):074506-5. PMID: PMC2737815.
9. Snyder CJ, DelaBarre L, Metzger GJ, van de Moortele PF, Akgun C, Ugurbil K, Vaughan JT. Initial results of cardiac imaging at 7 Tesla. *Magn Reson Med.* 2009;61(3):517-24. PMID: 2939145.
10. Vaughan JT, Snyder CJ, DelaBarre LJ, Bolan PJ, Tian J, Bolinger L, Adriany G, Andersen P, Strupp J, Ugurbil K. Whole-body imaging at 7T: Preliminary results. *Magnetic Resonance in Medicine.* 2009;61(1):244-8. PMID: 2875945.

11. Adriany G, Auerbach EJ, Snyder CJ, Gozubuyuk A, Moeller S, Ritter J, Van de Moortele PF, Vaughan T, Ugurbil K. A 32-Channel Lattice Transmission Line Array for Parallel Transmit and Receive MRI at 7 Tesla. *Magnetic Resonance in Medicine*. 2010;63(6):1478-85. PMID: 2946833.
12. Deelchand DK, Van de Moortele PF, Adriany G, Iltis I, Andersen P, Strupp JP, Vaughan JT, Ugurbil K, Henry PG. In vivo ¹H NMR spectroscopy of the human brain at 9.4 T: initial results. *J Magn Reson*. 2010;206(1):74-80. PMID: 2940249.
13. Metzger GJ, van de Moortele PF, Akgun C, Snyder CJ, Moeller S, Strupp J, Andersen P, Shrivastava D, Vaughan T, Ugurbil K, Adriany G. Performance of external and internal coil configurations for prostate investigations at 7 T. *Magn Reson Med*. 2010;64(6):1625-39. PMID: 2991410.
14. Shrivastava D, Abosch A, Hanson T, Tian J, Gupte A, Iaiizzo PA, Vaughan JT. Effect of the extracranial deep brain stimulation lead on radiofrequency heating at 9.4 Tesla (400.2 MHz). *J Magn Reson Imaging*. 2010;32(3):600-7. PMID: 2933930.
15. Wu X, Akgun C, Vaughan JT, Andersen P, Strupp J, Ugurbil K, Van de Moortele PF. Adapted RF pulse design for SAR reduction in parallel excitation with experimental verification at 9.4 T. *J Magn Reson*. 2010;205(1):161-70. PMID: 2919242.
16. Wu X, Vaughan JT, Ugurbil K, Van de Moortele PF. Parallel excitation in the human brain at 9.4 T counteracting k-space errors with RF pulse design. *Magn Reson Med*. 2010;63(2):524-9.
17. Snyder C, DelaBarre L, Moeller S, Akgun C, Van de Moortele P-F, Bolan P, Ugurbil K, Vaughan JT, Metzger G. Comparison Between Eight- and Sixteen-Channel TEM Transceive Arrays for Body Imaging at 7 Tesla. *Magn Reson Med*. 2011; Accepted with Revisions.
18. Suttie JJ, DelaBarre L, Pitcher A, van de Moortele P-F, Dass S, Snyder CJ, Francis JM, Metzger GJ, Weale P, Ugurbil K, Neubauer S, Robson M, Vaughan T. 7 Tesla (T) human cardiovascular magnetic resonance imaging using FLASH and SSFP to assess cardiac function: validation against 1.5 T and 3 T. *NMR in Biomedicine*. in press.
19. Shrivastava D, Hanson T, Kulesa J, Tian J, Gregor A, Vaugahn JT. Radiofrequency heating in porcine models with a 'large' 32 cm internal diameter, 7T (296 MHz) head coil. *Magn Reson Med*. (accepted with minor revisions).
20. Tian J, Shrivastava D, Vaughan JT. A simplified head model for local SAR evaluation at ultra-high fields. *Phys Med Biol*. In review.
21. Tian J, Snyder C, Liu W, Collins C, Gopinath A, Vaughan JT. B1, SNR, and SAR Variation with Head Size in MRI. *Magn Reson Med*. Article under review.
22. Shrivastava D, Schlentz R, Kulesa J, Gallagher W, Snyder C, DelaBarre L, Hanson T, Iaiizzo P, Vaughan JT. MR Safety Measurements. *CMRR Workshop; 2007; 6th Bi-Annual 2007 Minnesota Workshops, Minneapolis, USA*.

2. Peer Reviewed Abstracts and Conference Publications

23. Van de Moortele P-F, Snyder C, DelaBarre L, Adriany G, Vaughan T, Ugurbil K. Calibration Tools for RF Shim at Very High Field with Multiple Element RF Coils: From Ultra Fast Local Relative Phase to Absolute Magnitude B_1^+ Mapping. Proceedings 15th Scientific Meeting, International Society for Magnetic Resonance in Medicine; 2007 May 19-25, 2007; Berlin, DE.
24. Goerke U, Bolan P, Akgun C, Adriany G, Snyder C, van de Moortele P, DelaBarre L, Harel N, Vaughan T, Ugurbil K, Ellermann J. Ultrahigh magnetic field imaging of the knee using a transmit/receive array coil. Proceedings 16th Scientific Meeting, International Society for Magnetic Resonance in Medicine; April; Toronto 2008.
25. Shrivastava D, DelaBarre L, Hanson T, Vaughan JT. Improved MR Thermometry to Measure Brain Temperatures. ASME - Summer Bioengineering Conference, ; Marco Island, USA 2008.
26. Shrivastava D, DelaBarre L, Michaeli S, Snyder C, Hanson T, Vaughan J. Proton Resonance Frequency Shift Based NMR Thermometry for Ultra-High Field RF Safety Appl. Proceedings 16th Scientific Meeting, International Society for Magnetic Resonance in Medicine; April; Toronto 2008.
27. Shrivastava D, Schlentz R, Kulesa J, DelaBarre L, Snyder C, Hanson T, Vaughan J. 9.4 T RF Heating: In Vivo Thermoregulatory Temperature Response in Porcine Models. Proceedings 16th Scientific Meeting, International Society for Magnetic Resonance in Medicine; April; Toronto 2008.
28. Shrivastava D, Schlentz R, Kulesa J, DelaBarre L, Snyder C, Hanson T, Vaughan JT. Identification of Possibly Unsafe RF Exposure Thresholds for Humans using Porcine Models. ASME-SBC; 2008; ASME - Summer Bioengineering Conference, Marco Island, USA, 2008.
29. Snyder C, DelaBarre L, Metzger G, Akgun C, Bolan P, Ugurbil K, Vaughan T. Separate Transmit and Receive Arrays for 7T Body Imaging. Proceedings 16th Scientific Meeting, International Society for Magnetic Resonance in Medicine; 2008 April; Toronto.
30. Vaughan J, al. e. Whole Body Imaging at 7T with a 16 Channel Body Coil and B1 Shimming. Proceedings 16th Scientific Meeting, International Society for Magnetic Resonance in Medicine; 2008; Toronto.
31. Vaughan T, DelaBarre L, Snyder C, Mangia S, Tian J, Waks M, Shillak S, Petropoulos L, Adriany G, Andersen P, Strupp J, Ugurbil K. Whole Body Imaging at 7T with a 16 Channel Body Coil and B1 Shimming. Proceedings 16th Scientific Meeting, International Society for Magnetic Resonance in Medicine; 2008 April; Toronto.
32. Adriany G, Deelchand DK, Henry P-G, Tian J, Vaughan JT, K. U, Van de Moortele PF. A 16 channel T/R Open-Faced Head Array for Humans at 9.4T. Proc 17th Annual ISMRM; Honolulu,Hawaii,USA 2009.
33. Akgun C, DelaBarre L, Goerke U, Snyder C, Ellerman J, Ugurbil K, Vaughan J. Multi-channel transceive coil for improved knee imaging at 7T. Proceedings 17th Scientific Meeting, International Society for Magnetic Resonance in Medicine; April; Honolulu 2009.

34. Akgun C, DelaBarre L, Snyder C, Tian J, Gopinath A, Ugurbil K, Vaughan J. Alternating Impedance Element for 7T Multi-Channel Transceive Coil. Proceedings 17th Scientific Meeting, International Society for Magnetic Resonance in Medicine; April; Honolulu 2009.
35. Akgun CE, DelaBarre L, Sung-Min S, Snyder C, Adriany G, Ugurbil K, Vaughan JT, Gopinath A. Novel multi-channel transmission line coil for high field magnetic resonance imaging. Microwave Symposium Digest, 2009 MTT '09 IEEE MTT-S International 2009.
36. DelaBarre L, Weale p, Snyder C, van de Moortele P, Metzger G, Zuehlsdorff S, Nielles-Vallespin S, Bolan P, Auerbach E, Ugurbil K, Jerecic R, Vaughan J. Cardiac Cine: Advances at 7T. Proceedings 17th Scientific Meeting, International Society for Magnetic Resonance in Medicine; April; Honolulu 2009.
37. Metzger G, Moeller S, Snyder C, Ugurbil K, van de Moortele P, Adriany G. Endorectal Combined Surface Array for Prostate Imaging at 7T. Proceedings 17th Scientific Meeting, International Society for Magnetic Resonance in Medicine; April; Honolulu 2009.
38. Metzger GJ, Weale P, DelaBarre LJ, Bolan PJ, Zuehlsdorff S, Nielles-Vallespin S, Van de Moortele PF, Snyder CJ, Auerbach E, Vaughan JT, Ugurbil K, Jerecic R. Exploring the Promise Land of 7T for CMR with T-PAT accelerated imaging techniques - First Results for Real Time Cardiac Function and Tagging in Volunteers. Society for Cardiovascular Magnetic Resonance; Orlando, FL 2009.
39. Shrivastava D, Hanson T, Abosch A, Vaughan JT. RF Heating due to a Deep Brain Stimulation Electrode at 9.4 T (400.2 MHz) in Porcine Heads. Proceedings 17th Scientific Meeting, International Society for Magnetic Resonance in Medicine; ISMRM, Honolulu, Hawaii, USA 2009.
40. Shrivastava D, Hanson T, Kulesa J, Vaughan JT. RF safety and thermal characteristics of porcine heads after euthanasia. ISMRM; Hawaii, Honolulu 2009.
41. Shrivastava D, Liimatainen T, Goerke U, Kulesa J, Hanson T, Michaeli S, Vaughan JT. Optimized signal intensity and T1r based NMR thermometry for ultra-high field RF safety applications. Proceedings 17th Scientific Meeting, International Society for Magnetic Resonance in Medicine; Honolulu, Hawaii 2009.
42. Snyder C, DelaBarre L, Tian J, Akgun C, Metzger G, Moeller S, Ugurbil K, Vaughan J. Using Separated Volume Transmit and Local Receiver Arrays for Body Imaging at 7T. Proceedings 17th Scientific Meeting, International Society for Magnetic Resonance in Medicine; 2009 April; ISMRM, Honolulu, HI, USA.
43. Van de Moortele P, Auerbach E, Ugurbil K, Ritter J. Multiple Area B1 Shimming: An efficient, low SAR approach for T2-weighted fMRI acquired in the Visual and Motor Cortices of the Human Brain at Ultra-High Field. Proceedings 17th Scientific Meeting, International Society for Magnetic Resonance in Medicine; 2009 April; Honolulu.
44. Van de Moortele P, Ugurbil K. Very Fast Multi Channel B1 Calibration at High Field in the Small Flip Angle Regime. Proceedings 17th Scientific Meeting, International Society for Magnetic Resonance in Medicine; 2009 April; Honolulu.

45. Vaughan J, Snyder C, Delabarre L, Tian J, Adriany G, Andersen P, Strupp J, Ugurbil K. Clinical Imaging at 7T with a 16 Channel Whole Body Coil and 32 Receive Channels. Proceedings 17th Scientific Meeting, International Society for Magnetic Resonance in Medicine; 2009 April; Honolulu.
46. Vaughan JT. 7T CMR. Society for Cardiovascular Magnetic Resonance; 2009; Orlando, FL.
47. Wu X, Deelchand D, Yarnykh V, Ugurbil K, Van de Moortele P. Actual Flip Angle Imaging: From 3D to 2D. Proceedings 17th Scientific Meeting, International Society for Magnetic Resonance in Medicine; 2009 April; Honolulu.
48. Wu X, Powell N, Marjanska M, Garwood M, Ugurbil K, Van de Moortele P. A Flexible Design Algorithm for Single-shot 2D Circular/Elliptical OVS RF Pulses. Proceedings 17th Scientific Meeting, International Society for Magnetic Resonance in Medicine; 2009 April; Honolulu.
49. Wu X, Vaughan J, Ugurbil K, Van de Moortele P. Correction of Parallel Transmit RF pulses at 9.4 T Using Measured Gradient Waveforms. Proceedings 17th Scientific Meeting, International Society for Magnetic Resonance in Medicine; 2009 April; Honolulu.
50. Wu X, Vaughan J, Ugurbil K, Van de Moortele P. Implementation of VERSE Parallel Transmission at 9.4 T. Proceedings 17th Scientific Meeting, International Society for Magnetic Resonance in Medicine; 2009 April; Honolulu.
51. Yoo H, Gopinath A, Vaughan J. RF B1 field localization at 9.4T through convex optimization with an iterative method. Proceedings 17th Scientific Meeting, International Society for Magnetic Resonance in Medicine; 2009 April; Honolulu.
52. Adriany G, Harel N, Yacoub E, Moeller S, Ghose G, Ugurbil K. A 21 channel Transceiver Array for Non-human Primate Applications at 7 Tesla. Proc 18th ISMRM; Stockholm, Sweden 2010.
53. Adriany G, Ritter J, Van de Moortele PF, Vaughan JT, K. U. Experimental verification of enhanced B1 Shim performance with a Z-encoding RF coil array at 7 tesla. Proc 18th Annual ISMRM; Stockholm, Sweden 2010.
54. Akgun CE, DelaBarre LJ, Snyder CJ, Adriany G, Gopinath A, Ugurbil K, Vaughan JT. RF Field Profiling Through Element Design for High Field Volume Coils. Proceedings 18th Scientific Meeting, International Society for Magnetic Resonance in Medicine; Stockholm, Sweeden 2010.
55. Akgun CE, DelaBarre LJ, Snyder CJ, Sohn S-M, Adriany G, Ugurbil K, Gopinath A, Vaughan JT. Alternating Impedance Multi-Channel Transmission Line Resonators for High Field Magnetic Resonance Imaging. IEEE Microwave Theory and Techniques International Microwave Symposium; Anaheim, CA 2010.
56. DelaBarre LJ, Schillak S, Tramm B, Snyder CJ, Vaughan JT. Separated Volume Transmit / Volume Receive Arrays for Use in a 7T Head Gradient. Proceedings 18th Scientific Meeting, International Society for Magnetic Resonance in Medicine; Stockholm, Sweeden 2010.
57. Shrivastava D, Goerke U, Porter D, Vaughan J. New developments in bioheat transfer modeling and MR thermometry to improve radiofrequency safety in high field and ultra-high field MRI. ISMRM - RF Safety Workshop; 2010; ISMRM - RF Safety Workshop, Stillwater, MN.

58. Shrivastava D, Hanson T, Kulesa J, Tian J, Gregor A, Vaugahn JT. Systemic radio-frequency heating in porcine models with a 12.5" diameter, 8 channel, 7 T (296 MHz) head coil. ISMRM; ISMRM, Stockholm, Sweden 2010.
59. Shrivastava D, Vaughan JT. Development of an Anatomically Accurate Porcine Head Model to Study Radiofrequency Heating due to MRI. Proceedings 18th Scientific Meeting, International Society for Magnetic Resonance in Medicine; 2010; Stockholm, Sweeden.
60. Snyder C, DelaBarre L, Tian J, Akgun C, Metzger GJ, Ugurbil K, Vaughan JT. 28-Channel Receive-Only Array for Body Imaging at 7T. Proceedings of the 19th Annual Meeting of ISMRM; Stockholm 2010.
61. Snyder C, DelaBarre L, Tian J, Akgun C, Vaughan JT. Using Piezoelectric Actuators for Remote Tuning of Transmit Coils. In: Proceedings of the 19th Annual Meeting of ISMRM; 2010; Stockholm.
62. Suttie JJ, DelaBarre L, Metzger GJ, van de Moortele PF, Snyder CJ, Weale P, Neubauer S, Robson MD, Vaughan JT. Clinical cardiac imaging at 7 Tesla: a validation study. Proceedings 18th Scientific Meeting, International Society for Magnetic Resonance in Medicine; 2010; Stockholm, SE.
63. Tian J, Snyder CJ, DelaBarre LJ, Vaughan JT. Using Dielectrics and RF Shielding to Increase B_1^+ Efficiency and Homogeneity. Proceedings 18th Scientific Meeting, International Society for Magnetic Resonance in Medicine; 2010; Stockholm, Sweeden.
64. Vaughan JT. Initial CMR Experience at 7T. Society for Cardiovascular Magnetic Resonance; 2010; Phoenix, AZ.
65. Vaughan JT, Snyder CJ, DelaBarre LJ, Ugurbil K. RF Coil Designs for 7T Cardiac Imaging. Proceedings 18th Scientific Meeting, International Society for Magnetic Resonance in Medicine; 2010; Stockholm, Sweeden.
66. Wu X, Schmitter S, Tian J, Vaughan JT, Ugurbil K, Van de Moortele PF. SAR analysis of Parallel Transmission in Cardiac Imaging at 7T. ISMRM - RF Safety Workshop; Stillwater, MN 2010.
67. Wu X, Vaughan JT, Ugurbil K, Van de Moortele PF. 16-channel parallel transmission in the human brain at 9.4 Tesla: Initial results. Proceedings 18th Scientific Meeting, International Society for Magnetic Resonance in Medicine; 2010; Stockholm, Sweeden.
68. Yoo H, Gopinath A, Vaughan JT. A Method to Control Non-uniformity RF B_1 Field for High Field Magnetic Resonance Imaging. IEEE Microwave Theory and Techniques International Microwave Symposium; 2010; Anaheim, CA.
69. Yoo H, Gopinath A, Vaughan JT. Rapid B_1 field calculation using integral equations for RF shimming. Proceedings 18th Scientific Meeting, International Society for Magnetic Resonance in Medicine; 2010; Stockholm, Sweeden.
70. DelaBarre LJ, Snyder CJ, Vaughan JT, van de Moortele PF. Balanced SSFP cardiac imaging at 7T. Proceedings 19th Scientific Meeting, International Society for Magnetic Resonance in Medicine; Montreal, Quebec 2011.

71. Demir T, DelaBarre L, Akin B, Adriany G, Ugurbil K, Atalar E. Optical Transmission System for High Field Systems. Proceedings 19th Scientific Meeting, International Society for Magnetic Resonance in Medicine; 2011; Montreal, Quebec.
72. Metzger GJ, DelaBarre LJ, Bi X, Shah S, Zuehlsdorff S, Vaughan JT, Ugurbil K, Van de Moortele PF. Left Coronary Artery Imaging at 7T: Initial Results using Multiple B1+ Shimming Algorithms and Targets. Proceedings 19th Scientific Meeting, International Society for Magnetic Resonance in Medicine; Montreal, Quebec 2011.
73. Shrivastava D, Goerke U, Michaeli S, Tian J, Abosch A, Vaughan JT. An MR Thermometry-GBHTM 'Hybrid' Model to Determine Radiofrequency Heating near Implanted Leads in High Field Imaging. Proceedings 19th Scientific Meeting, International Society for Magnetic Resonance in Medicine; Montreal, Quebec 2011.
74. Shrivastava D, Goerke U, Michaeli S, Tian J, DelaBarre LJ, Vaugahn JT. Total Proton Resonance Frequency Shift Coefficient in the Porcine Brain to Image Radiofrequency Heating in Ultra-high Field MRI. Proceedings 19th Scientific Meeting, International Society for Magnetic Resonance in Medicine; Montreal, Quebec 2011.
75. Shrivastava D, Kulesa J, Tian J, Adriany G, DelaBarre LJ, Vaugahn JT. Radio-Frequency Heating in Swine with an 8 Channel, 7 T (296 MHz) Head Coil. Proceedings 19th Scientific Meeting, International Society for Magnetic Resonance in Medicine; Montreal, Quebec 2011.
76. Shrivastava D, Tian J, Abosch A, Vaughan JT. Radio-Frequency Heating at Deep Brain Stimulation Lead Electrodes due to Imaging with Head Coils in 3 T and 7T. Proceedings 19th Scientific Meeting, International Society for Magnetic Resonance in Medicine; 2011; Montreal, Quebec.
77. Snyder C, DelaBarre L, Metzger G, Ugurbil K, Vaughan JT. 32-Channel Receive Only Array for Cardiac Imaging at 7T. Proceedings of the 19th Annual Meeting of the ISMRM; Montreal 2011.
78. Snyder C, Rogers C, DelaBarre L, Robson M, Vaughan JT. Remote Tuning and Matching an 8-Channel Transceive Array at 7T. Proceedings of the 19th Annual Meeting of ISMRM; Montreal 2011.
79. Sohn S-M, Gopinath A, Vaughan JT. Electrically auto-tuned RF coil design. Proceedings 20th Scientific Meeting, International Society for Magnetic Resonance in Medicine; 2011; Montreal, Quebec.
80. Tian J, Vaughan JT. Tailoring RF Power Distribution for Body Torso MRI at 300MHz. Proceedings 19th Scientific Meeting, International Society for Magnetic Resonance in Medicine; Montreal, Quebec 2011.
81. Vaughan JT, Myer D. RF Coil Element Mounted Power Amplifiers. Proceedings 19th Scientific Meeting, International Society for Magnetic Resonance in Medicine; 2011; Montreal, Quebec.

5.3. Patents

82. Adriany G, Van de Moortele P-F, Ritter J, Voje W, Vaughan JT, Ugurbil K, inventors; Regents of the University of Minnesota, assignee. Spatially reconfigurable magnetic resonance coil USA. 2009.
83. Akgun CE, Snyder C, DelaBarre L, Moeller S, Van de Moortele P-F, Vaughan JT, Ugurbil K, inventors; Regents of the University of Minnesota, assignee. Three dimensional RF coil structures for field profiling 2009.
84. Olson CC, Vaughan JT, Gopinath A, inventors; Regents of the University of Minnesota, assignee. Radio frequency field localization for magnetic resonance USA patent 7,633,293. 2009.
85. Snyder CJ, Vaughan JT, inventors; Remotely adjustable reactive and resistive electrical element and method. Appl. 61/158345 2009.
86. Vaughan JT, inventor Regents of the University of Minnesota, assignee. RF Coil for Imaging Systems and Methods of Operation. USA patent US 2009/0237077 A1. 2009.
87. Vaughan JT, Ugurbil K, Adriany G, inventors; Regents of the University of Minnesota, assignee. Radio frequency gradient, shim and parallel imaging coil. USA. 2009.
88. Vaughan JT, Adriany G, Snyder C, Akgun CE, Tian J, Ugurbil K, Van de Moortele P-F, Moeller S, inventors; Regents of the University of Minnesota, assignee. Multi-current elements for magnetic resonance radio frequency coils USA patent 7,710,117. 2010.
89. Vaughan JT, Van de Moortele P-F, DelaBarre L, Olson CC, Orser H, Gopinath A, Ugurbil K, Snyder C, Adiany G, Akgun CE, Tian J, Strupp J, Andersen PM, Wu X, inventors; Regents of the University of Minnesota assignee. High field magnetic resonance patent 7,800,368. 2010.
90. Vaughan JT, Tian J, inventors; Regents of the University of Minnesota, assignee. Coil Element Decoupling for MRI. 2010.
91. Vaughan JT, Adriany G, Ugurbil K, inventors; Regents of the University of Minnesota, assignee. Assymmetric radio frequency magnetic line array 2011.

4. Invited Book Chapters

92. Shrivastava D, Goerke U, Porter D, Vaughan, JT, "New Developments in Bioheat Transfer Modeling and MR Thermometry to Improve Radiofrequency Safety in High-field and Ultra-high Field MRI," RF Safety Handbook, ISMRM publisher, (2011)
93. Shrivastava D, Vaughan JT, "Radiofrequency Heating Measurements and Models," in Encyclopedia of Magnetic Resonance, John Wiley and Sons, 2010.
94. Shrivastava D, Vaughan JT, "Radiofrequency Heating Measurements and Models," in RF Coil Handbook, John Wiley and Sons, 2011.

95. Vaughan JT, Shrivastava D, "RF Propagation and Loss in the Human Loaded RF Coil" RF Safety Handbook, ISMRM publisher (2011)
96. Vaughan JT. "The Parallel Transceiver for MRI" Encyclopedia of Magnetic Resonance, John Wiley and Sons, (2011)
97. Vaughan JT. "The Parallel Transceiver for MRI" RF Coil Handbook, John Wiley and Sons, (2011)
98. Vaughan JT, "TEM Coils for MRI" Encyclopedia of Magnetic Resonance, John Wiley and Sons, (2011)
99. Vaughan JT, "TEM Coils for MRI"RF Coils Handbook, John Wiley and Sons, (2011)

5. Books, Encyclopedia Sections, Journal Editions

100. RF Coil Handbook, J Thomas Vaughan, John Griffiths Editors, John Wiley and Sons (2011)
101. Encyclopedia of Magnetic Resonance, RF Coils, J Thomas Vaughan (2011)
102. RF Coils for MRI, NMR in Biomedicine, Special Edition (2010)
103. RF Safety Handbook, J Thomas Vaughan, International Society for Magnetic Resonance in Medicine (2011)

Works Cited

1. Ogawa S, Menon RS, Tank DW, Kim SG, Merkle H, Ellermann JM, Ugurbil K. Functional brain mapping by blood oxygenation level-dependent contrast magnetic resonance imaging. A comparison of signal characteristics with a biophysical model. *Biophys J*. 1993;64(3):803-12. PMID: 1262394.
2. Yacoub E, Shmuel A, Pfeuffer J, Van de Moortele PF, Adriany G, Andersen P, Vaughan JT, Merkle H, Ugurbil K, Hu XP. Imaging brain function in humans at 7 Tesla. *Magn Reson Med*. 2001;45(4):588-94.
3. Yacoub E, Van De Moortele PF, Shmuel A, Ugurbil K. Signal and noise characteristics of Hahn SE and GE BOLD fMRI at 7 T in humans. *Neuroimage*. 2005;24(3):738-50.
4. Pfeuffer J, van de Moortele PF, Yacoub E, Shmuel A, Adriany G, Andersen P, Merkle H, Garwood M, Ugurbil K, Hu X. Zoomed functional imaging in the human brain at 7 Tesla with simultaneous high spatial and high temporal resolution. *Neuroimage*. 2002;17(1):272-86.
5. Menon RS, Ogawa S, Hu X, Strupp JP, Anderson P, Ugurbil K. BOLD based functional MRI at 4 Tesla includes a capillary bed contribution: echo-planar imaging correlates with previous optical imaging using intrinsic signals. *Magn Reson Med*. 1995;33(3):453-9.
6. Hu X, Le TH, Ugurbil K. Evaluation of the early response in fMRI in individual subjects using short stimulus duration. *Magn Reson Med*. 1997;37(6):877-84.
7. Menon RS, Ogawa S, Strupp JP, Ugurbil K. Ocular dominance in human V1 demonstrated by functional magnetic resonance imaging. *J Neurophysiol*. 1997;77(5):2780-7.
8. Yacoub E, Harel N, Ugurbil K. High-field fMRI unveils orientation columns in humans. *Proc Natl Acad Sci U S A*. 2008;105(30):10607-12. PMID: 2492463.
9. Yacoub E, Shmuel A, Pfeuffer J, Van De Moortele PF, Adriany G, Ugurbil K, Hu X. Investigation of the initial dip in fMRI at 7 Tesla. *NMR Biomed*. 2001;14(7-8):408-12.
10. Yacoub E, Duong TQ, Van De Moortele PF, Lindquist M, Adriany G, Kim SG, Ugurbil K, Hu X. Spin-echo fMRI in humans using high spatial resolutions and high magnetic fields. *Magn Reson Med*. 2003;49(4):655-64.
11. Shmuel A, Yacoub E, Chaimow D, Logothetis NK, Ugurbil K. Spatio-temporal point-spread function of fMRI signal in human gray matter at 7 Tesla. *Neuroimage*. 2007;35(2):539-52.
12. Ugurbil K, Kim DS, Duong T, Hu XP, Ogawa S, Gruetter R, Chen W, Kim SG, Zhu XH, Yacoub E, Van de Moortele PF, Shmuel A, Pfeuffer J, Merkle H, Andersen P, Adriany G. Magnetic resonance imaging of brain function and neurochemistry. *Proceedings of the Ieee*. 2001;89(7):1093-106.
13. Kim DS, Ronen I, Olman C, Kim SG, Ugurbil K, Toth LJ. Spatial relationship between neuronal activity and BOLD functional MRI. *Neuroimage*. 2004;21(3):876-85.
14. Pfeuffer J, Adriany G, Shmuel A, Yacoub E, Van De Moortele PF, Hu X, Ugurbil K. Perfusion-based high-resolution functional imaging in the human brain at 7 Tesla. *Magn Reson Med*. 2002;47(5):903-11.
15. Zhu XH, Kim SG, Andersen P, Ogawa S, Ugurbil K, Chen W. Simultaneous oxygenation and perfusion imaging study of functional activity in primary visual cortex at different visual stimulation frequency: quantitative correlation between BOLD and CBF changes. *Magn Reson Med*. 1998;40(5):703-11.
16. Duong TQ, Kim DS, Ugurbil K, Kim SG. Localized cerebral blood flow response at submillimeter columnar resolution. *Proc Natl Acad Sci U S A*. 2001;98(19):10904-9. PMID: 58572.
17. Zhao F, Wang P, Hendrich K, Ugurbil K, Kim SG. Cortical layer-dependent BOLD and CBV responses measured by spin-echo and gradient-echo fMRI: insights into hemodynamic regulation. *Neuroimage*. 2006;30(4):1149-60.
18. Bolan PJ, Yacoub E, Garwood M, Ugurbil K, Harel N. In vivo micro-MRI of intracortical neurovasculature. *Neuroimage*. 2006;32(1):62-9.
19. Gruetter R, Weisdorf SA, Rajanayagan V, Terpstra M, Merkle H, Truwit CL, Garwood M, Nyberg SL, Ugurbil K. Resolution improvements in in vivo H-1 NMR spectra with increased magnetic field strength. *J Magn Reson*. 1998;135(1):260-4.

20. Ugurbil K, Adriany G, Andersen P, Chen W, Garwood M, Gruetter R, Henry PG, Kim SG, Lieu H, Tkac I, Vaughan T, Van de Moortele PF, Yacoub E, Zhu XH. Ultrahigh field magnetic resonance imaging and spectroscopy. *Magn Reson Imaging*. 2003;21(10):1263-81.
21. Mangia S, Tkac I, Gruetter R, Van de Moortele PF, Maraviglia B, Ugurbil K. Sustained neuronal activation raises oxidative metabolism to a new steady-state level: evidence from ¹H NMR spectroscopy in the human visual cortex. *J Cereb Blood Flow Metab*. 2007;27(5):1055-63.
22. Mangia S, Tkac I, Gruetter R, Van De Moortele PF, Giove F, Maraviglia B, Ugurbil K. Sensitivity of single-voxel ¹H-MRS in investigating the metabolism of the activated human visual cortex at 7 T. *Magn Reson Imaging*. 2006;24(4):343-8.
23. Mangia S, Tkac I, Logothetis NK, Gruetter R, Van de Moortele PF, Ugurbil K. Dynamics of lactate concentration and blood oxygen level-dependent effect in the human visual cortex during repeated identical stimuli. *J Neurosci Res*. 2007;85(15):3340-6.
24. Tkac I, Andersen P, Adriany G, Merkle H, Ugurbil K, Gruetter R. In vivo ¹H NMR spectroscopy of the human brain at 7 T. *Magn Reson Med*. 2001;46(3):451-6.
25. Zhang N, Zhu XH, Lei H, Ugurbil K, Chen W. Simplified methods for calculating cerebral metabolic rate of oxygen based on ¹⁷O magnetic resonance spectroscopic imaging measurement during a short ¹⁷O₂ inhalation. *J Cereb Blood Flow Metab*. 2004;24(8):840-8.
26. Lei H, Ugurbil K, Chen W. Measurement of unidirectional Pi to ATP flux in human visual cortex at 7 T by using in vivo ³¹P magnetic resonance spectroscopy. *Proc Natl Acad Sci U S A*. 2003;100(24):14409-14. PMID: 283605.
27. Choi IY, Tkac I, Ugurbil K, Gruetter R. Noninvasive measurements of [1-(¹³C)]glycogen concentrations and metabolism in rat brain in vivo. *J Neurochem*. 1999;73(3):1300-8.
28. Vaughan JT, Garwood M, Collins CM, Liu W, DelaBarre L, Adriany G, Andersen P, Merkle H, Goebel R, Smith MB, Ugurbil K. 7T vs. 4T: RF power, homogeneity, and signal-to-noise comparison in head images. *Magn Reson Med*. 2001;46(1):24-30.
29. Vaughan T, DelaBarre L, Snyder C, Tian J, Akgun C, Shrivastava D, Liu W, Olson C, Adriany G, Strupp J, Andersen P, Gopinath A, van de Moortele PF, Garwood M, Ugurbil K. 9.4T Human MRI: Preliminary Results. *Magn Reson Med*. 2006;56(6):1274-82.
30. Rooney WD, Johnson G, Li X, Cohen ER, Kim SG, Ugurbil K, Springer CS, Jr. Magnetic field and tissue dependencies of human brain longitudinal ¹H₂O relaxation in vivo. *Magn Reson Med*. 2007;57(2):308-18.
31. Duong TQ, Yacoub E, Adriany G, Hu XP, Ugurbil K, Vaughan JT, Merkle H, Kim SG. High-resolution, spin-echo BOLD, and CBF AM at 4 and 7 T. *Magn Reson Med*. 2002;48(4):589-93.
32. Shmuel A, Yacoub E, Pfeuffer J, Van de Moortele PF, Adriany G, Hu X, Ugurbil K. Sustained negative BOLD, blood flow and oxygen consumption response and its coupling to the positive response in the human brain. *Neuron*. 2002;36(6):1195-210.
33. Duong TQ, Yacoub E, Adriany G, Hu X, Ugurbil K, Kim SG. Microvascular BOLD contribution at 4 and 7 T in the human brain: gradient-echo and spin-echo fMRI with suppression of blood effects. *Magn Reson Med*. 2003;49(6):1019-27.
34. Duong TQ, Yacoub E, Adriany G, Hu XP, Andersen P, Vaughan JT, Ugurbil K, Kim SG. Spatial specificity of high-resolution, spin-echo BOLD, and CBF fMRI at 7 T. *Magn Reson Med*. 2004;51(3):646-7.
35. Yacoub E, Shmuel A, Logothetis N, Ugurbil K. Robust detection of ocular dominance columns in humans using Hahn Spin Echo BOLD functional MRI at 7 Tesla. *Neuroimage*. 2007;37(4):1161-77. PMID: 2040323.
36. Wiesinger F, Van De Moortele PF, Adriany G, De Zanche N, Ugurbil K, Pruessmann KP. Parallel imaging performance as a function of field strength - An experimental investigation using electrodynamic scaling. *Magn Reson Med*. 2004;52(5):953-64.
37. Wiesinger F, Van de Moortele PF, Adriany G, De Zanche N, Ugurbil K, Pruessmann KP. Potential and feasibility of parallel MRI at high field. *NMR Biomed*. 2006;19(3):368-78.

38. Moeller S, Van de Moortele PF, Goerke U, Adriany G, Ugurbil K. Application of parallel imaging to fMRI at 7 Tesla utilizing a high 1D reduction factor. *Magn Reson Med.* 2006;56(1):118-29.
39. Snyder CJ, DelaBarre L, Metzger GJ, van de Moortele PF, Akgun C, Ugurbil K, Vaughan JT. Initial results of cardiac imaging at 7 Tesla. *Magn Reson Med.* 2009;61(3):517-24. PMID: 2939145.
40. Vaughan T, Snyder C, DelaBarre L, Bolinger L, Tian J, Andersen P, Strupp J, Adriany G, Ugurbil K. 7T Body Imaging: First Results. Proceedings 14th Scientific Meeting, International Society for Magnetic Resonance in Medicine; 2006 May; Seattle, WA.
41. Vaughan JT, Adriany G, Garwood M, Yacoub E, Duong T, DelaBarre L, Andersen P, Ugurbil K. Detunable transverse electromagnetic (TEM) volume coil for high-field NMR. *Magn Reson Med.* 2002;47(5):990-1000.
42. Vaughan JT, Adriany G, Snyder C, Tian J, Thiel T, Bolinger L, Liu H, DelaBarre L, Ugurbil K. Efficient high-frequency body coil for high-field MRI. *Magn Reson Med.* 2004;52:851-9.
43. Vaughan JT, Snyder CJ, DelaBarre LJ, Bolan PJ, Tian J, Bolinger L, Adriany G, Andersen P, Strupp J, Ugurbil K. Whole-body imaging at 7T: Preliminary results. *Magn Reson Med.* 2009;61(1):244-8. PMID: 2875945.
44. Vaughan JT, Adriany G, Garwood M, Yacoub E, Duong T, DelaBarre L, Andersen P, Ugurbil K. A Detunable Volume Coil for High Field NMR. *Magn Reson Med.* 2002;47(5):990-1000.
45. Adriany G, Van de Moortele P-F, Wiesinger F, Moeller S, Strupp J, Andersen P, Snyder C, Zhang X, Chen W, Pruessmann K, Boesiger P, Vaughan J, Ugurbil K. Transmit and receive transmission line arrays for 7 tesla parallel imaging. *Magn Reson Med.* 2005;53(2):434-45.
46. Adriany G, Auerbach EJ, Snyder CJ, Gozubuyuk A, Moeller S, Ritter J, Van de Moortele PF, Vaughan T, Ugurbil K. A 32-Channel Lattice Transmission Line Array for Parallel Transmit and Receive MRI at 7 Tesla. *Magn Reson Med.* 2010;63(6):1478-85. PMID: 2946833.
47. Adriany G, Van de Moortele PF, Ritter J, Moeller S, Auerbach EJ, Akgun C, Snyder CJ, Vaughan T, Ugurbil K. A geometrically adjustable 16-channel transmit/receive transmission line array for improved RF efficiency and parallel imaging performance at 7 Tesla. *Magn Reson Med.* 2008;59(3):590-7.
48. Van de Moortele PF, Akgun C, Adriany G, Moeller S, Ritter J, Collins CM, Smith MB, Vaughan JT, Ugurbil K. B₁ destructive interferences and spatial phase patterns at 7 T with a head transceiver array coil. *Magn Reson Med.* 2005;54(6):1503-18.
49. Metzger GJ, Snyder C, Akgun C, Vaughan T, Ugurbil K, Van de Moortele PF. Local B₁₊ shimming for prostate imaging with transceiver arrays at 7T based on subject-dependent transmit phase measurements. *Magn Reson Med.* 2008;59(2):396-409.
50. Wu X, Akgun C, Vaughan JT, Andersen P, Strupp J, Ugurbil K, Van de Moortele PF. Adapted RF pulse design for SAR reduction in parallel excitation with experimental verification at 9.4 T. *J Magn Reson.* 2010;205(1):161-70. PMID: 2919242.
51. Wu X, Vaughan JT, Ugurbil K, Van de Moortele PF. Parallel excitation in the human brain at 9.4 T counteracting k-space errors with RF pulse design. *Magn Reson Med.* 2010;63(2):524-9.
52. Deelchand DK, Van de Moortele PF, Adriany G, Iltis I, Andersen P, Strupp JP, Vaughan JT, Ugurbil K, Henry PG. In vivo 1H NMR spectroscopy of the human brain at 9.4 T: initial results. *J Magn Reson.* 2010;206(1):74-80. PMID: 2940249.
53. SEMCAD X, Reference Manual for the SEMCAD X Simulation Platform for Electromagnetic compatibility, antenna design, and dosimetry. Version 11.0. 2006.
54. Shrivastava D, Vaughan JT. A Generic Bioheat Transfer Thermal Model for a Perfused Tissue. *Journal of Biomechanical Engineering.* 2009;131(7):074506-5. PMID: PMC2737815.
55. Shrivastava D, Vaughan JT. Development of an Anatomically Accurate Porcine Head Model to Study Radiofrequency Heating due to MRI. Proceedings 18th Scientific Meeting, International Society for Magnetic Resonance in Medicine; 2010; Stockholm, Sweden.
56. Dewhirst MW, Viglianti BL, Lora-Michiels M, Hanson M, Hoopes PJ. Basic principles of thermal dosimetry and thermal thresholds for tissue damage from hyperthermia. *Int J Hyperthermia.* 2003;19(3):267-94.

57. Vaughan JT, Tian J, inventors; Regents of the University of Minnesota, assignee. Coil Element Decoupling for MRI. 2010 22 April 2010.
58. Pruessmann KP, Weiger M, Scheidegger MB, Boesiger P. SENSE: Sensitivity encoding for fast MRI. *Magn Reson Med.* 1999;42(5):952-62.
59. Insko E, Bolinger L. Mapping of the Radiofrequency Field”, *JMR Series A*, 102, 82-85 (1993). *J Magn Reson A.* 1993;102:82-5.
60. Kellman P, McVeigh ER. Image reconstruction in SNR units: a general method for SNR measurement. *Magn Reson Med.* 2005;54(6):1439-47.
61. Snyder C, DelaBarre L, Moeller S, Akgun C, Van de Moortele P-F, Bolan P, Ugurbil K, Vaughan JT, Metzger G. Comparison Between Eight- and Sixteen-Channel TEM Transceive Arrays for Body Imaging at 7 Tesla. *Magn Reson Med.* 2011; Accepted with Revisions.
62. Snyder C, DelaBarre L, Tian J, Akgun C, Vaughan JT. Using Piezoelectric Actuators for Remote Tuning of Transmit Coils. In: *Proceedings of the 19th Annual Meeting of ISMRM; 2010; Stockholm.*
63. Snyder C, Rogers C, DelaBarre L, Robson M, Vaughan JT. Remote Tuning and Matching an 8-Channel Transceive Array at 7T. *Proceedings of the 19th Annual Meeting of ISMRM; Montreal, Quebec 2011.*
64. Snyder CJ, Vaughan JT, inventors; Remotely adjustable reactive and resistive electrical element and method. *Appl.* 61/158345 2009.
65. Collins CM, Liu WZ, Wang JH, Gruetter R, Vaughan JT, Ugurbil K, Smith MB. Temperature and SAR calculations for a human head within volume and surface coils at 64 and 300 MHz. *J Magn Reson Imaging.* 2004;19(5):650-6.